Title

Therapeutically viable generation of neurons with antisense oligonucleotide suppression of PTB

Journal

Nature Neuroscience, 24(8)

ISSN

1097-6256

Authors

Maimon, Roy
Chillon-Marinas, Carlos
Snethlage, Cedric E
et al.

Publication Date

2021-08-01

DOI

10.1038/s41593-021-00864-y

Peer reviewed

HHS Public Access

Author manuscript

Nat Neurosci. Author manuscript; available in PMC 2022 February 01.

Published in final edited form as:

Nat Neurosci. 2021 August ; 24(8): 1089–1099. doi:10.1038/s41593-021-00864-y.

Therapeutically viable generation of neurons with antisense oligonucleotide suppression of PTB

Roy Maimon[#1,2], **Carlos Chillon-Marinas**[#1,2], **Cedric E Snethlage**[3], **Sarthak M Singhal**[4], **Melissa McAlonis-Downes**[1,2], **Karen Ling**[6], **Frank Rigo**[6], **C. Frank Bennett**[6], **Sandrine Da Cruz**[1,7], **Thomas S. Hnasko**[4,5], **Alysson R. Muotri**[2,3], **Don W. Cleveland**[1,2]

[1]Ludwig Institute for Cancer Research, University of California at San Diego, La Jolla, CA, USA

[2]Department of Cellular and Molecular Medicine, University of California at San Diego, La Jolla, CA, USA

[3]Department of Pediatrics, Rady Children's Hospital San Diego, Stem Cell Program, Center for Academic Research and Training in Anthropogeny (CARTA), Kavli Institute for Brain and Mind, University of California San Diego, La Jolla, CA, USA

[4]Department of Neurosciences, University of California at San Diego, La Jolla, CA, USA

[5]Veterans Affairs San Diego Healthcare System, San Diego, CA, USA

[6]Ionis Pharmaceuticals, Carlsbad, CA, USA

[7]VIB-KU Leuven Center for Brain & Disease Research and Department of Neurosciences, KU Leuven, Leuven, Belgium

[#] These authors contributed equally to this work.

Abstract

Methods to enhance adult neurogenesis by reprogramming glial cells into neurons enable production of new neurons in the adult nervous system. Development of therapeutically viable approaches to induce new neurons is now required to bring this concept to clinical application. Here, we successfully generate new neurons in the cortex and dentate gyrus of the aged adult mouse brain by transiently suppressing Polypyrimidine-Tract-Binding-Protein-1 (PTB) using an antisense-oligonucleotide (ASO) delivered by a single injection into cerebral spinal fluid. Radial glial-like cells and other GFAP-expressing cells convert into new neurons that over a two-month period acquire mature neuronal character in a process mimicking normal neuronal maturation. The

Author for correspondence Don W. Cleveland, Ludwig Institute for Cancer Research, Dept. of Cellular and Molecular Medicine, Mail Code 0660, Univ. of California at San Diego, 9500 Gilman Drive, La Jolla, CA 92093-0660, Tel 858-534-7811; Fax 858-534-7659, dcleveland@health.ucsd.edu.

Author Contribution Statement

R.M., C.C.M., S.D.C., and D.W.C. conceived the study. R.M., C.C.M., C.E.S, S.M.S., K.L., F.R., C.F.B., S.D.C., T.H., A.R.M., and D.W.C. designed the study. R.M., C.C.M, C.E.S., S.M.S., M.M.D., and K.L. performed the experiments. R.M., C.C.M., S.M.S., analyzed the data. R.M., C.C.M, C.E.S, S.M.S, F.R., C.F.B., S.D.C., T.H., A.R.M., and D.W.C. wrote the manuscript; all authors discussed the results and commented on the manuscript.

Competing Interest Statement

C.F.B., F.R., and K.L. are employees of, and D.W.C. is a consultant for, Ionis Pharmaceuticals. A.R.M. is a co-founder and has an equity interest in TISMOO, a company dedicated to genetic analysis and brain organoid modeling focusing on therapeutic applications customized for autism spectrum disorder and other neurological disorders with genetic origins. The terms of this arrangement have been reviewed and approved by the University of California San Diego by its conflict of interest policies.

new neurons functionally integrate into endogenous circuits and modify mouse behavior. Thus, generation of new neurons in the dentate gyrus of the aging brain can be achieved with a therapeutically feasible approach, thereby opening prospects for production of neurons to replace those lost to neurodegenerative disease.

Introduction:

For years it was believed that neurons that compose the central nervous system (CNS) are not replaceable. This notion was formally stated[1] in 1928 by Santiago Ramon y Cajal: “In the adult centers, the neural paths are something fixed and immutable: everything may die, nothing may be regenerated”, albeit he added that “It is for the science of the future to change, if possible, this harsh decree.” Since then, techniques to enhance the generation of a wide range of neural cells in the adult brain have been heavily studied during the past two decades[2,3].

Two main strategies to generate new neurons in the adult brain have been pursued: 1) enhancing adult neurogenesis from neuronal progenitors[4] and 2) reprogramming (or direct conversion) of non-neuronal-cells into neurons[5], a process also known as transdifferentiation. Initial efforts made use of combinatorial expression of neural-lineage-specific transcription factors to convert non-neurons, including fibroblasts and astrocytes, into electrically active neurons without passing through a stem cell state[3,6] (reviewed in ref. [7]). Three groups[8,9,10] simplified this approach, reporting direct conversion of glia into neurons by using focally injected adeno-associated virus (AAV) to chronically lower expression of a single target, Polypyrimidine Tract Binding Protein 1 (PTB), an RNA binding protein.

Starting with a model of chemically-induced Parkinson’s-like disease in mice, Qian et al.[8] focally suppressed PTB levels within the mouse substantia nigra by stimulating catalytic degradation of its mRNA mediated by stereotactic injection either of 1) an AAV encoding an shRNA to PTB mRNA or 2) a PTB-targeting antisense oligonucleotide (ASO). Focal reduction in PTB in chemically induced Parkinson’s-like disease in mice converted astrocytes or other GFAP-expressing cells into new nigral neurons, enabling sustained Parkinson’s-like disease reversal[8]. A similar glia to neuron conversion was reported following stereotactic injection (into either the sub-retina or the striatum) of an AAV encoding a CRISPR-CasRx protein and a guide RNA targeting PTB mRNA[9]. Moreover, sustained, focal PTB reduction in striatal oligodendrocytes was reported to facilitate their conversion into neurons[10]. Thus, chronic PTB reduction in different glial cell lineages, including astrocytes[8,9], Muller glia cells[9], radial glial cells[11], and oligodendrocytes[12], may lead to conversion into neurons in young adult mice.

ASO injection into cerebral spinal fluid (CSF) is a therapeutically viable approach that was initiated 14 years ago[13] and validated to yield effective delivery to neurons and glial cells throughout the rodent[13] and non-human primate[14] nervous systems. ASO injection is a current standard of care for the fatal childhood disease spinal muscular atrophy[15] and is in five ongoing Phase I trials in ALS, Parkinson’s, and Alzheimer’s diseases and in Phase III trials for inherited ALS from a mutation in superoxide dismutase[16,17] and for Huntington’s

disease[18]. Recognizing that neither PTB-mediated conversion nor any other method for enhancing neurogenesis or promoting transdifferentiation has been achieved using an approach that is proven to be therapeutically viable, we now test if generation of new functional cortical or hippocampal neurons can be achieved in the normal aging adult nervous system by transiently suppressing PTB synthesis with single dose ASO injection into CSF.

Results

ASO-dependent generation of new neurons in a human organoid model

Recognizing that introduction of 2 or more mismatches abrogates activity of RNase H dependent ASOs[19], we used the Bowtie algorithm to identify 196 candidate 20mer ASOs with 100% complementarity to both human and murine PTB pre-mRNAs and which did not match any other region within the human or murine genomes even with allowing a 2 base mismatch. We identified those which most effectively reduced PTB mRNA levels in a mouse cell line with effective ASO uptake (murine 4T1 cells) and then conducted a preliminary toxicity assay after intracerebroventricular (ICV) injection into CSF of healthy adult mice to determine that each was well tolerated with no overt changes in body weight, overall health, spontaneous activity, and gross motor behavior observed. At necropsy, this included measurement (by qPCR) of expression of neuroinflammatory markers in CNS tissues.

Two top candidate ASOs (Figure 1a) were identified based upon suppression of PTB mRNA levels in cell culture (Figure 1b) and tolerability (Extended Data Figure 1a). Reduction of PTB mRNA was observed 72 hours post ICV injection, followed by induction of neuronal PTB (nPTB) 15 days post injection (Extended Data Figure 1b,c). The addition of either ASO to culture media of primary murine astrocytes rapidly suppressed PTB mRNA (Figure 1c). Within 3 days, conversion into neurons was initiated, with reduced PTB expression accompanied by a sharp reduction in GFAP-encoding mRNA (an astrocytic marker) and induction of the neuronal-specific NeuN mRNA (Figure 1c).

Human brain organoids are emerging as a scaled-down, three-dimensional model of the human brain, mimicking various developmental features, including generation of new neurons by their conversion from radial glia[20] and incorporation into neuronal network[21]. We used this model to test the impact of PTB-ASOs on the generation of new neurons. Recognizing that the use of ASOs to modulate gene expression in human organoids has not previously been reported, we initially added a fluorescently tagged ASO targeting the long non-coding RNA Malat1 to brain organoid culture media and monitored its free uptake and efficacy over time. Widespread Malat1-ASO presence was observed within the organoids, accompanied by 85% reduction of Malat1 mRNA levels at both 2- and 4-weeks post-treatment (Extended Data Figure 2).

We then tested whether ASO-dependent reduction of PTB expression would result in the formation of additional neurons in the human brain organoids (Figure 1d). PTB-ASOs penetrated the organoids (Figure 1e) and reduced PTB mRNA levels (Figure 1f). Reduction in GFAP mRNA was coupled with induction of NeuN mRNA (Figure 1f), similar to what was found after PTB suppression in cultured mouse astrocytes (Figure 1b). The number of

cells expressing the neuronal protein marker NeuN was slightly elevated (Figure 1g,h). Furthermore, axons and dendrites (measured by axonal marker Tuj1 (Extended Data Figure 3a,b) or dendritic marker MAP2 (Figure 1i,j,k,l)) were significantly elevated in PTB-ASO treated organoids compared with control ASO treated organoids. Neither the number (Extended Data Figure 3c,d) of pluripotent cells (SOX2+) nor those with caspase 3 activation (Extended Data Figure 3e) was changed by PTB-ASO treatment. Hence, new neurons were induced by reduction in PTB expression in human brain organoids mediated by free uptake of an ASO to trigger catalytic degradation of PTB mRNA.

PTB ASO conversion of GFAP-expressing cells into neurons in the adult mouse brain

To test whether new neurons could be generated in the young adult mammalian brain via ASO administration, we introduced a PTB-ASO into the cerebral spinal fluid (CSF) by single-dose intracerebroventricular (ICV) injection. To monitor potential generation of new neurons, we used congenic C57b/6 mice carrying 1) a GFAP-promoted Cre^{ERT2}-recombinase transgene such that Cre recombinase will be expressed in GFAP expressing cells and activated by tamoxifen-dependent nuclear import of Cre^{ERT2} and 2) a chicken β-actin-promoted gene (CAG-lox-stop-lox-tdTomato) encoding a red fluorescent protein (tdTomato) whose expression will be permanently activated by the action of Cre^{ERT2} removal of a “lox-stop-lox” cassette preceding the tdTomato coding sequence[22] even if the GFAP-expressing cell changes identity into a neuron (Figure 2a).

Tamoxifen-mediated induction of Cre^{ERT2} activity was initiated in adult GFAP-Cre^{ERT2}, CAG-lox-stop-lox-tdTomato mice followed by injection into CSF of either saline or a control ASO. Two months later, at the age of 5 months, exhaustive examination of the cortex from each saline injected control mouse (n=3) revealed ~0.1% of Td-tomato expressing cells also expressing NeuN, an outcome consistent with leaky expression of Cre^{ERT2} within a small number of pre-existing neurons. Single injection into CSF of a PTB mRNA-targeting ASO induced a 10 fold higher increase in NeuN expressing tdTomato+ cells in the first and fourth layers of the cortex (Figure 2b), each displaying a neuronal morphology similar to endogenous cortical neurons (Figure 2c). It also induced a similar increase in neurons in the CA1 region of the hippocampus, which developed a morphology expected of pyramidal neurons (Extended Data Figure 4).

The dentate gyrus of the hippocampus is the brain region where the most active neurogenesis has been documented to take place[23–25]. Radial glial cells, stem cell precursors, and astrocytes - all reported to express GFAP (reviewed in ref.[26]) - are found in the dentate gyrus[2,27,28]. In tamoxifen-induced GFAP-Cre^{ERT2}, CAG-lox-stop-lox-tdTomato mice, 0.4% of the tdTomato-expressing cell population also expressed NeuN+ two months after saline or control ASO injection into CSF (Figure 2d), consistent with the known low rate of ongoing neurogenesis in the dentate gyrus of young adult mice[29].

In sharp contrast, two months after PTB-ASO injection (at a final age of 5 months), an obvious increase in tdTomato+, NeuN+ neurons was identified in the granular layer of the dentate gyrus (Figure 2d; Supplementary Videos 1&2). Unbiased counting of total tdTomato + expressing cells throughout the dentate gyrus revealed a 37.5-fold increase (compared with saline or control ASO injected mice) in newly generated neurons identified as tdTomato+,

NeuN+ cells, with 15% (± 5%, n=3) of total tdTomato+ cells also NeuN+ (Figure 2d,e,f, Supplementary Video 3). Counting also revealed that only 25.5% (±4.9%, n=7) of endogenous GFAP-expressing astrocytes expressed tdTomato. Correcting for this, we calculated that newly induced neurons comprise 7.8% of the total neurons of the granular cell layer (GCL) in the entire dentate gyrus of these 5 months old mice (Figure 2g).

PTB ASO generation of new neurons in the aged adult mouse brain

It is well accepted that neurogenesis sharply decreases in the aged mammalian nervous system[29–31], with no new neurons detectable in mice by 10 months of age[29,31]. Using the same approach as used in 5 months old mice (Figure 2a), we injected either PTB or a control ASO intraventricularly into CSF of 1-year-old GFAP-Cre^{ERT2}, CAG-lox-stop-lox-tdTomato mice and then monitored the degree of neuronal generation two months post-administration. As expected, without PTB suppression no new neurons were detected in the dentate gyrus of these aged mice (Extended Data Figure 5). With PTB ASO injection, limited new neuron formation was observed in the cortex of these aged mice (Extended Data Figure 6), at a rate similar to what was seen in younger mice. Remarkably, single PTB-ASO injection into CSF produced new neurons that comprised 4.5% of the total neurons in the dentate gyri of aged (14 months old) mice (Figure 2d,g), with conversion of 5% of all tdTomato-positive cells into tdTomato+, NeuN+ expressing neurons (Figure 2f).

The robust conversion rates in the hippocampi of our experimental models raised the question of whether new neurogenesis depleted the GFAP-expressing cell pool[32]. In the hippocampus of adult mice, almost all (97%) of tdTomato-expressing neurons did not accumulate detectable levels of GFAP two months after ASO injection (Figure 3a,b). Conversion to neurons did not, however, affect the pool of GFAP-expressing cells, as no difference was observed in the total number of GFAP or nestin expressing cells in the human organoid model (Figure 3c) or in GFAP-positive cells in the dentate gyri of PTB-ASO treated animals (Figure 3c,d,e). Instead, Ki67, a marker for cell proliferation[33], was elevated in the dentate gyri of both 5 month or 1.2 year old PTB-ASO injected mice (Extended Data Figure 7a-c) and in PTB-treated human brain organoids (Extended Data Figure 7d), consistent with proliferation of precursor cells stimulated to divide by homeostatic mechanisms that maintain the levels of glia, including astrocytes[32].

Thus, a single ICV injection of an ASO to suppress PTB induces new neurons in the dentate gyrus of the adult mouse brain with no depletion in total GFAP-expressing cell number.

Newly generated hippocampal neurons undergo canonical neuronal development

The process by which newly generated neurons in normal development are incorporated into the granular cell layer is well established and involves expression of specific markers and development of defined neuronal morphology[24,26,34,35]. Recognizing this, we monitored newly generated neurons at an early time (1 week and 2 weeks) after ICV injection of PTB ASOs, times when newly developing neurons (but not mistakenly labeled, pre-existing neurons) would be expected to be immature[24,26,34]. At these early time points, most of the tdTomato expressing cells with neuronal character in hippocampi of PTB-ASO treated mice had morphological characteristics expected of newly generated neurons. They were located

exclusively in the basal layer of the dentate gyrus and exhibited shorter and less complex dendritic branches (Figure 4a,c) than those of tdTomato expressing neurons at 2 months post ASO injection (Figure 4a,d), the latter of which had acquired dendritic morphologies similar to those of mature, endogenous neurons[34–36].

Furthermore, one and two weeks after PTB ASO injection into 5 month old mice, doublecortin (DCX), a protein expressed in developing immature neurons, but silenced as those neurons mature[37], was present in 26.3 and 49.2 times (respectively) as many cells as found 1 and 2 weeks after injection of a control ASO (Figure 4b,e). Over a subsequent six week period, DCX-positive neurons in PTB ASO injected mice decreased by three fold (Figure 4b,e), as expected if many initial DCX-positive neurons had matured. Consistent with this interpretation, two weeks following ICV injection with PTB-ASO in 1.2 year old mice, many DCX positive cells were present, while there was a complete absence of DCX positive cells present in any of the age matched, control ASO injected mice (Figure 4e, Extended Data Figure 8). Indeed, in 1.2 year old PTB-ASO injected mice there was a 19.8 fold increase in DCX positive cells even when compared with control ASO injected young adult (5 month old) mice in which some endogenous neurogenesis was still occurring. PTB-mediated production of new neurons was also supported by a PTB-ASO-dependent increase in DCX in brain organoids (Extended Data Figure 9).

By 2 months post-ICV injection, the vast majority (92.7%) of tdTomato+ cells with neuronal morphology no longer expressed DCX, 97% of which had converted to expression of the mature neuronal marker NeuN (Figure 4d, Extended Data Figure 10). In comparison to the short dendritic branching in immature neurons present 2 weeks post-ICV of PTB-ASO (Figure 4a,d), after an additional six weeks the tdTomato+ neurons had developed long dendritic processes which extended into the Perforant pathway (Figure 4f,g) and contained MAP2 (Supplementary video 4), a marker for mature dendrites[38]. There was also a 16-fold increase over control ASO injected mice in tdTomato-positive+ axons extending from neurons in the dentate gyrus into the Mossy fiber path (Figure 4f,h,i) and into the hippocampal CA3 area (Figure 4f,j), consistent with successful integration into the hippocampal circuit.

Thus, PTB ASO-dependent generation of new neurons appears to trigger the typical maturation process by which new neurons are generated during development[39] and adult[40] neurogenesis.

Radial glial-like cells are the main cell population to convert into hippocampal neurons post transient PTB reduction

An unresolved controversy[41] is whether the apparent generation of new neurons from astrocytes in earlier reports[7] may actually reflect endogenous neuronal precursors or mature neurons mistakenly labeled by various fluorescent marking schemes, as opposed to transdifferentiation from glia. As mature astrocytes are well established[42] to accumulate starburst bundles of GFAP filaments that fill the central cell bodies (e.g., see Figure 3a), we determined that no DCX-containing immature neuron present in dentate gyri one week and two weeks after PTB ASO injection contained GFAP bundles (Figure 5a,b; Supplementary video 5). However, ~30% of the tdTomato+ cells exhibited morphologic characteristics

expected of radial glial cells (Figure 5a,c) [including triangular shaped cell bodies located near the sub granular zone and bushy radial dendrites extending through the granular cell layer[26]] but had hybrid neuronal/glial character, with a DCX+ cell body sharing dendrites with GFAP filaments, as would be expected for cells in the midst of conversion from radial glial-like cells into neurons (Figure 5c,d) (Supplementary video 6).

PTB ASO-induced neurons integrate into endogenous neuronal circuits

We next tested the electrical properties of the newly generated neurons. Immature neurons in dentate gyrus receive only excitatory GABA inputs, whereas mature neurons receive both inhibitory and excitatory glutamate inputs[24]. Electrophysiological recordings obtained from tdTomato-positive neurons in the granule cell layer of the dentate gyrus (Figure 6a) revealed spontaneous excitatory postsynaptic currents (sEPSCs) and spontaneous inhibitory postsynaptic currents (sIPSCs), indicating the presence of afferent glutamate and GABA synaptic inputs, respectively (Figure 6b), that were indistinguishable from endogenous tdTomato-negative neurons. Furthermore, current injections into tdTomato-positive neurons provoked action potentials similar to those from tdTomato-negative cells (Figure 6c). Measurement of other intrinsic membrane properties were also consistent with tdTomato-positive cells possessing membrane properties indistinguishable from neighboring tdTomato-negative cells (Table 1). These results indicate that within two months post-ICV injection of PTB-ASO into CSF newly generated neurons are sufficiently integrated into endogenous circuits to be capable of receiving both glutamate and GABA inputs and firing action potentials that are indistinguishable from the neighboring endogenous granular cell layer neurons.

PTB ASO-induced new neurons in the dentate gyrus are functional

Assays thought to rely on hippocampal related behaviors[43–45] were performed two months post ASO delivery to test the functionality of PTB ASO generated new neurons in the dentate gyri of 1.5 year old control or PTB ASO ICV injected mice. Using observers blinded to the treatment ASO, no differences between PTB and control ASO treated groups were seen in stress related behaviors[46] in open field assays that included distance traveled, velocity of movement, and time spent in the open (Figure 7a,b,c). Similarly, there were no differences between the two treatment groups in an optomotor assay (Figure 7d). However, using a Barnes maze test that scored the time required to find an escape hole during four days of training, as well as a final fifth day[44], the PTB-ASO treated group escaped the maze more rapidly compared to the control ASO-treated group (Figure 7e). Using a novel object recognition test[45] to monitor hippocampal function, a significant enhancement was recorded in the time spent near novel objects in PTB-ASO injected mice compared to those injected with a control ASO (Figure 7f,g).

Discussion

We have generated new neurons in the cortex and hippocampus of the normal aged adult mouse brain by a transient, partial suppression of PTB using an ASO delivered by a therapeutically viable single dose injection into CSF. While it is well known that the degree of neurogenesis dramatically decreases in aged mice[29–31], and that the number of neural

progenitors is depleted during aging[47], reduction in PTB triggered radial glial-like cells to convert into new granular neurons through what appears to be the typical developmental process by which new hippocampal neurons mature during development[39] and in young adult animals[40]. Over a two month period the new neurons acquire mature neuronal character and functionally integrate into endogenous circuits, with dendrites extending into the Perforant path and receiving inhibitory (GABA) and excitatory (glutamate) inputs, and axons extending into CA3 and sending action potentials which modify hippocampal-dependent mouse behavior. Suppression of PTB was also demonstrated to be sufficient to generate new human neurons in brain organoids in vitro.

Our evidence establishes that glial cells can switch identities to become new neurons in the healthy adult mouse brain. We determined this initially using a tamoxifen-inducible GFAP-Cre^{ERT2} transgene to permanently activate expression of a tdTomato gene reporter in GFAP-expressing cells, a well accepted approach to follow astrocyte-to-neuron conversion and one broadly used previously to claim conversion of astrocytes into neurons[8] and one argued to be the most reliable system to monitor the generation of new neurons[41]. While we recognize that an alternative hypothesis has proposed that Cre synthesized by glia may be transferred into existing neurons and thereby artifactually mark those neurons as having converted from glia[41], five lines of evidence demonstrate that new neurons convert from radial glia or astrocytes, not from artifactual activation of the tdTomato reporter in neurons already present.

First, production of tdTomato expressing neurons was enhanced 37.5 times in the dentate gyrus (and 10 times in the cortex or CA1) of reporter mice in which PTB expression was reduced with a PTB targeting ASO. This strikingly enhanced production of new neurons is inconsistent with artifactual marking of mature neurons. Second, using a Cre/tdTomato glial marking system, we established that the tdTomato positive neurons generated in response to PTB ASO injection mature morphologically over a time course of one week to two months, rather than initially appearing as the morphologically mature neurons that would be produced by artifactually marking existing neurons. Third, PTB suppression in the human organoid model, a well-established *in vitro* model of neurodevelopment, induced 50–100% increase in new neurons. Fourth, independent of Cre/tdTomato marking, PTB ASO injection into the adult mouse nervous system generated a transient 49.2 fold increase in new immature (DCX-positive) neurons 2 weeks post suppression of PTB. Fifth, ASO-mediated transient suppression of PTB improved mouse memory (in Barnes maze and novel object recognition assays), an outcome consistent with production of new functional neurons, but inconsistent with existing neurons artifactually labeled with tdTomato.

In each example we document, the new neurons generated by a transiently lowered PTB level appear to derive from conversion of a glial progenitor, including at least two different progenitors (radial glia for granular neurons and human neurons in organoids; astrocytes for cortical and pyramidal neurons). It is notable that morphology of the newly generated neurons strongly depended on the brain region in which they were generated (Extended Data Figure 4), with the converted neurons acquiring morphologies matching that characteristic of granular, pyramidal, or cortical neurons, respectively, that are representative for neurons of each region. It seems highly likely that neuronal identity is determined (or at least affected)

by local cues produced within each specific brain region, and potentially by intrinsic gene expression within the glial cells that convert to neurons within each brain subarea. Future studies (including gene expression monitoring and proteomics) are now needed to identify the key determinants (glial cell intrinsic or environmental) that comprise such cues.

Our findings demonstrate that generating new neurons in the aging brain (especially within the dentate gyrus) can be achieved with a therapeutically feasible approach of ASO-mediated transient reduction in PTB. This discovery may represent a foundational first step for therapy development through production of neurons to replace those lost in neurodegenerative diseases of aging. What we have achieved thus far is likely to be only the tip of an iceberg, rather than setting a limit on what is achievable. The ASOs we used for this study are not clinical candidates. PTB suppression was less than 50% in most brain regions, while optimized ASOs to other targets have previously been shown to yield dose dependent target RNA suppression to 5% of initial level[13,14,48]. In the brain region where PTB was reduced by more than 50% (the hippocampus), we document robust glia-to-neuron conversion even in aged mice, suggesting that suppression by at least this amount may be required to initiate efficient conversion in other brain regions. Optimization to identify ASOs with minimal toxicity and maximal efficacy is now essential. Nevertheless, our findings strongly support that a therapeutically feasible pharmacological intervention with ASOs to transiently suppress PTB can facilitate generation of replacement neurons within the aged mammalian nervous system.

Extended Data

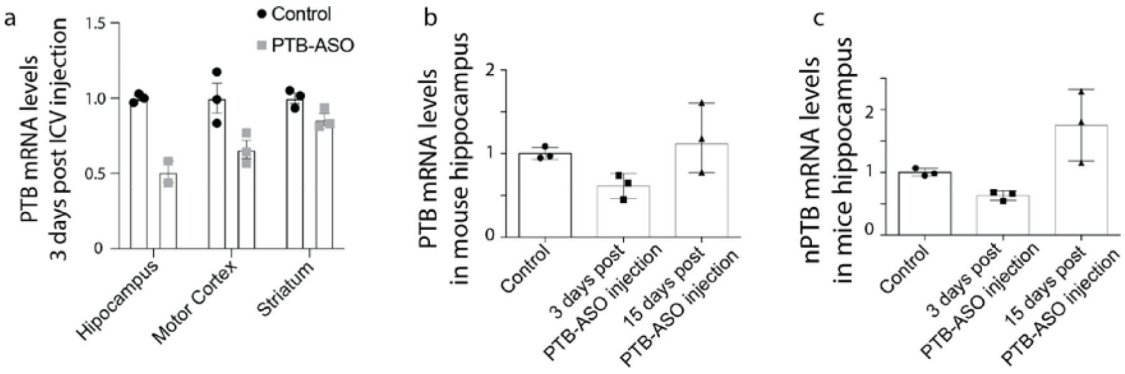

Extended Data Figure 1: PTB and neuronal PTB (nPTB) mRNA levels 3 days post-ICV injection of PTB-ASO2.

(a) PTB mRNA levels in the hippocampus, motor cortex, and striatum measured by qPCR, 3 days post ICV injection of 500 μg PTB or control ASOs into 3-months-old mouse brain. Data are presented as fold change mean +/− SEM (Hippocampus: control mean: 1 +/− 0.01; PTB-ASO mean: 0.5 +/− 0.07; n=3,n=2 biological repeats; respectively; Motor cortex: control mean: 1 +/− 0.09; PTB-ASO mean: 0.65 +/− 0.05; n=3 biological repeats; Striatum: control mean: 1 +/− 0.03; PTB-ASO mean: 0.86 +/− 0.04; n=3 biological repeats).

(b) PTB mRNA levels in the hippocampus measured by qPCR 3 days and 15 days post ICV injection of 500 mg PTB or control ASOs into 3-month-old mouse brain. Data are presented as fold change mean +/− SEM. (control mean: 1 +/− 0.04; 3 days post PTB-ASOs mean: 0.61 +/− 0.08; 15 days post PTB-ASOs mean: 1.18 +/− 0.24; n=3 biological repeats.

(c) Neuronal PTB (nPTB) mRNA levels in the hippocampus measured by qPCR 3 days and 15 days post ICV injection of 500 mg PTB or control ASOs into 3-month-old mouse brain. Data are presented as fold change mean +/− SEM (control mean: 1 +/− 0.03; 3 days post PTB-ASOs mean: 0.63 +/− 0.04; 15 days post PTB-ASOs mean: 1.75 +/− 0.33; n=3 biological repeats).

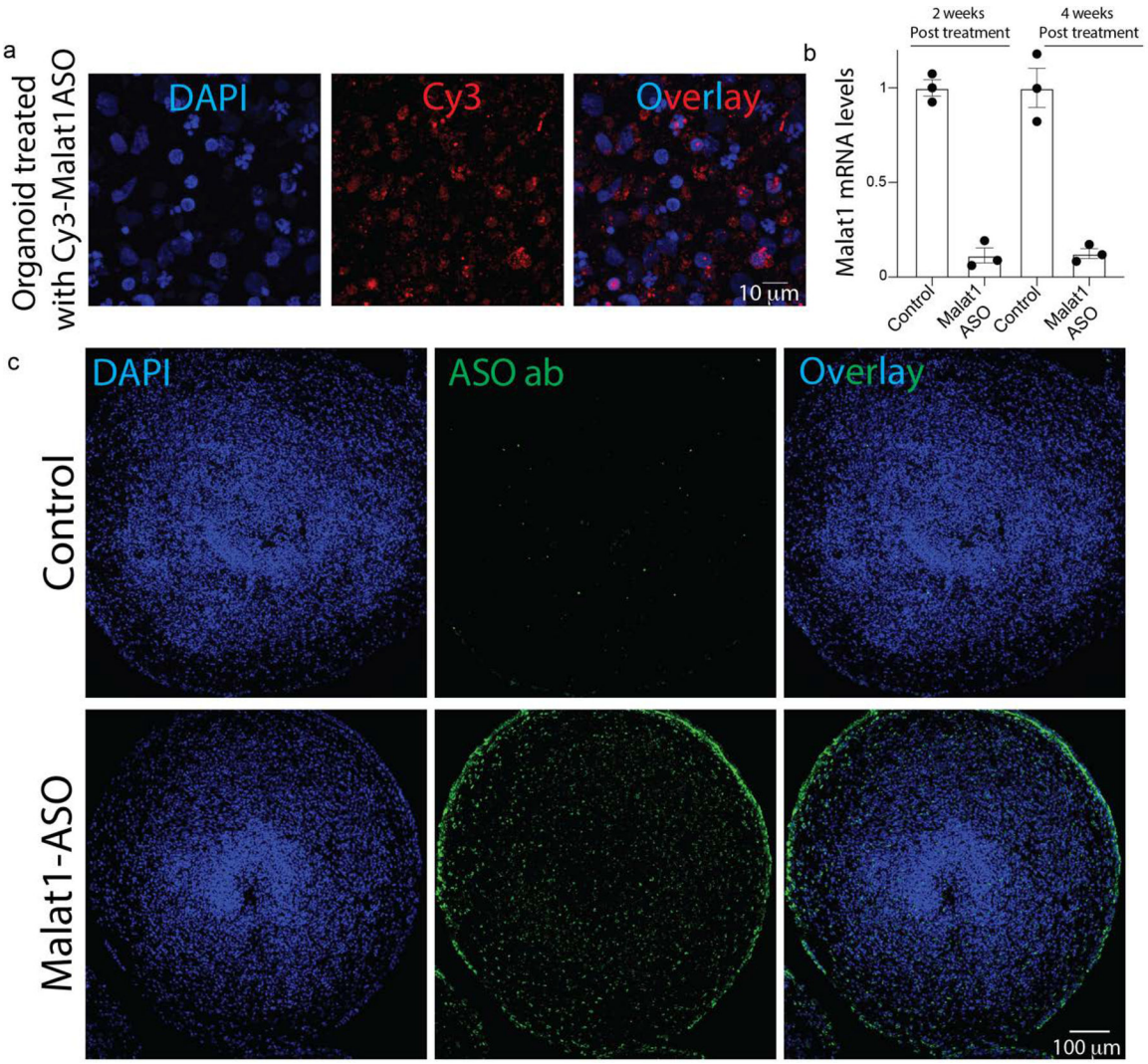

Extended Data Figure 2: ASOs efficiently penetrate into and regulate gene expression in 3D human organoids in culture.

(a) Representative immunofluorescence images from a 5-month-old human organoid taken 1-week post Cy3-Malat1-ASO addition to the culture medium. Images show a view of (*red*) Cy3-Malat1-ASO (visualized by direct immunofluorescence) or (*blue*) DAPI staining for DNA; experiment was reproduced two times, independently, with similar results.

(b) Malat1 mRNA levels measured by qPCR 2 or 4 weeks after addition to human organoid cultures or either 10 µM Malat1-ASO or control, non-targeting ASO. Data are presented as fold change mean +/− SEM (2 weeks control mean: 1 +/− 0.04; 2 weeks post Malat1-ASOs

mean: 0.11 +/− 0.03; 4 weeks control mean: 1 +/− 0.1; 4 weeks post Malat1-ASOs mean: 0.1 +/− 0.02; n=3 biological repeats).

(c) Representative immunofluorescence images from 5-month-old human organoids taken 1-month post-Malat1-ASO application to the organoid culture medium. Images show a view of (*green*) a Malat1-ASO (visualized by indirect immunofluorescence) or (*blue*) DAPI staining for DNA; experiment was reproduced three times, independently, with similar results.

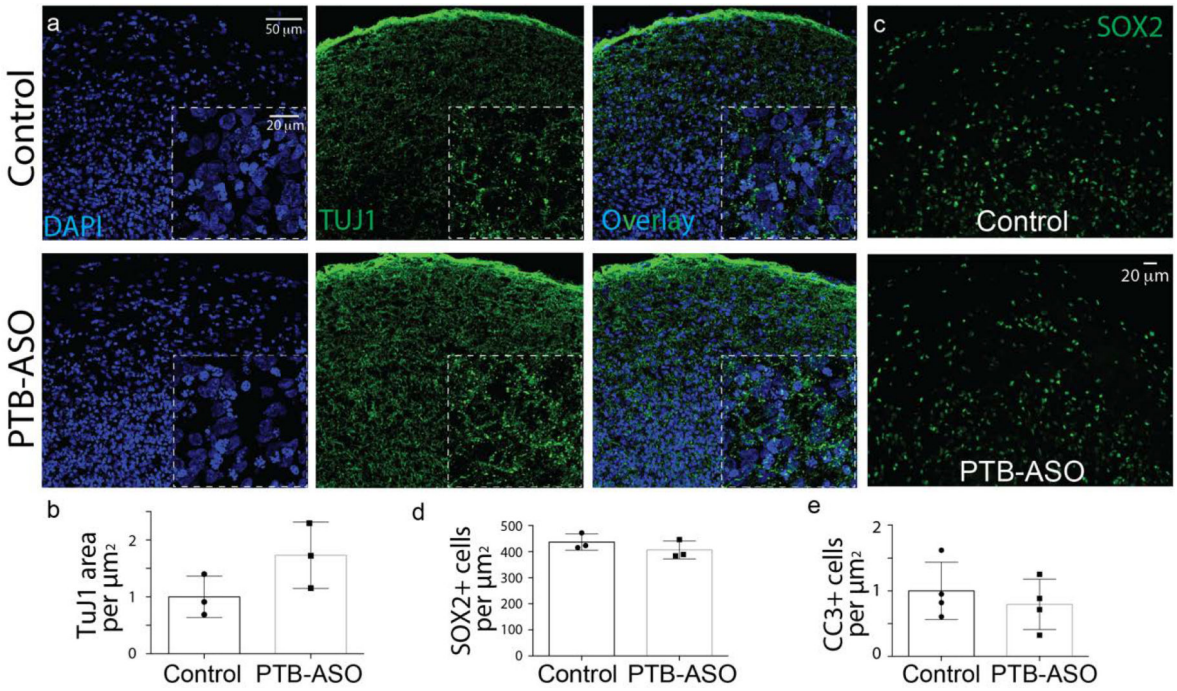

Extended Data Figure 3: PTB-ASO application into human organoid cultures leads to increase levels of TuJ1 protein with no alterations in SOX2 or caspase 3 markers.

(a) Representative immunofluorescences images of 5 months old human organoid taken 1-month post-PTB-ASO2 or control treatment. Images show a view of the axonal marker (*green*) TUJ1 (visualized by indirect immunofluorescence); DAPI staining for DNA; experiment was reproduced three times, independently, with similar results.

(b) Total TuJ1 area in PTB-ASO treated organoids compared to control ASO. Data are presented as fold change mean +/− SEM (control mean: 1 +/− 0.21; PTB-ASO mean: 1.73 +/− 0.33; n=3 biological repeats).

(c) Representative immunofluorescences images and from 5 months old human organoid taken 1-month post-PTB-ASO2 application to the culture medium. Images show a view of (*green*) SOX2 (visualized by indirect immunofluorescence); experiment was reproduced three times, independently, with similar results.

(d) Quantification of the total SOX2 positive cells per organoid area treated with PTB-ASO compared to ASO control. Data are presented as mean +/− SEM (control mean: 436.7 +/− 17.82; PTB-ASO mean: 406.3 +/− 19.89; n=3 biological repeats).

(e) Total caspase 3 (CC3) protein area in PTB-ASO treated organoids compared to control ASO. Data are presented as fold change mean +/− SEM (control mean: 1 +/− 0.21; PTB-ASO mean: 0.79 +/− 0.19; n=4 biological repeats).

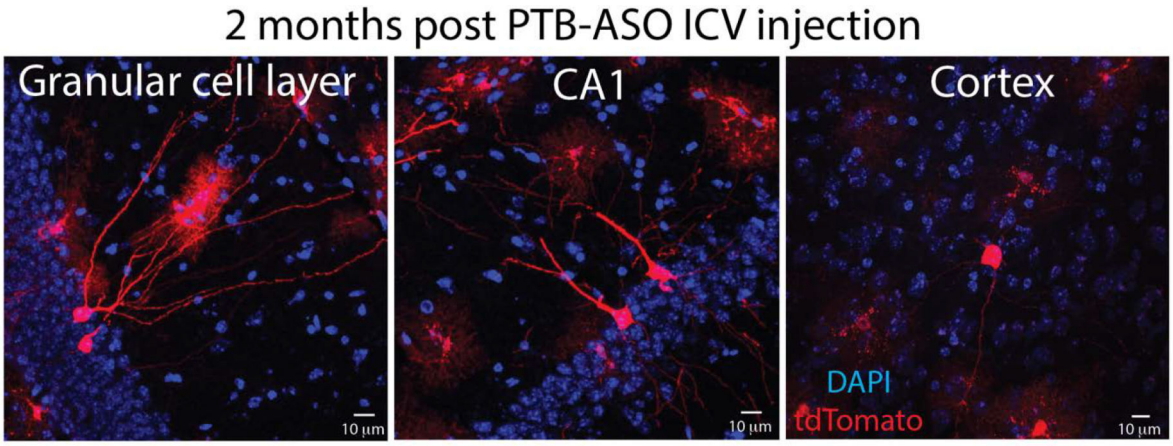

Extended Data Figure 4: Morphology of newly generated neurons in different brain regions, 2 months post-PTB-ASO ICV administration.

Representative immunofluorescence images of (*left*) granular cell layer, (*middle*) CA1, and (*right*) cortex, 2 months post-ICV injection of PTB-ASO2 into mice carrying both a CAG-lox-stop-lox-tdTomato gene and a tamoxifen-inducible GFAP-Cre^{ERT2} transgene. (*Red*) tdTomato (visualized by direct fluorescence); (*blue*) DAPI staining for DNA; experiment was reproduced three times, independently, with similar results.

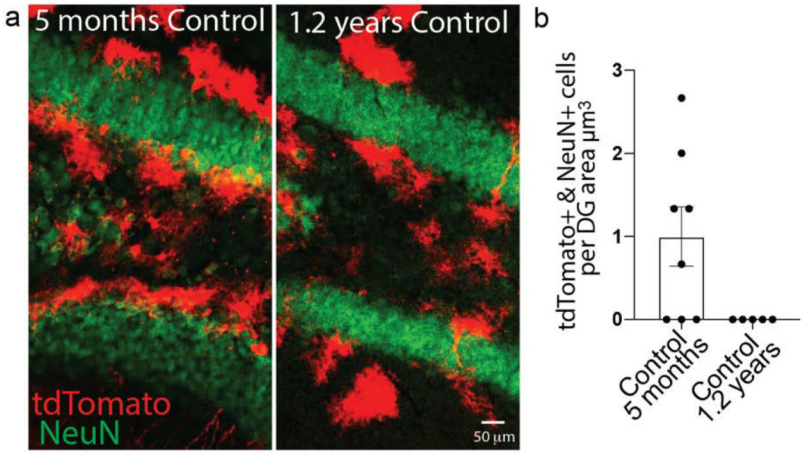

Extended Data Figure 5: New neurons along the dentate gyrus were not detected in 1.2 years old control injected mice.

(a) Representative immunofluorescence image from (*left*) 5 months and (*right*) 1.2 years old mouse dentate gyrus taken 2 months post-ICV injection of control-ASO into mice carrying both a CAG-lox-stop-lox-tdTomato gene and a tamoxifen-inducible GFAP-Cre^{ERT2} transgene. (*Green*) NeuN and (*red*) tdTomato (visualized by indirect immunofluorescence and direct fluorescence, respectively);

(b) Quantification of the tdTomato+ & NeuN+ neurons (iNeurons) in the granular cell layer 2 months post ICV injection of control-ASO at 5 months or 1.2 years old mice. Data are presented as fold change mean +/− SEM. (control 5 months mean: 1 +/− 0.35; Control 1.2 years old mean: 0 +/− 0; n=8, n=5 brain slides per each condition, n=3, n=1, respectively).

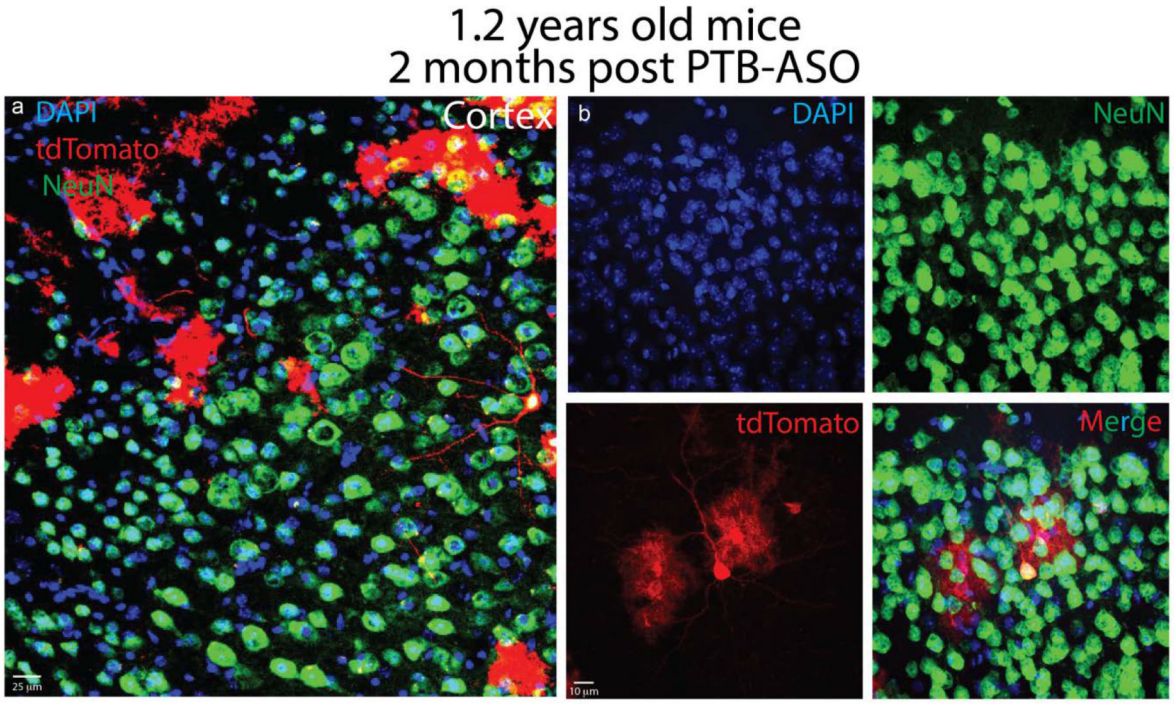

Extended Data Figure 6: Injection of ASO to suppress PTB into the cerebral spinal fluid induces a low number of new neurons in the aged mouse cortex.

(a,b) Representative immunofluorescence image **(a)** from 1.2 years old mouse cortex taken 2 months post-ICV injection of PTB-ASO2 into mice carrying both a CAG-lox-stop-lox-tdTomato gene and a tamoxifen-inducible GFAP-Cre^{ERT2} transgene. **(b)** high-magnification views of newly induced neurons (iNeurons) in the cortex expressing (*green*) NeuN and (*red*) tdTomato (visualized by indirect immunofluorescence and direct fluorescence, respectively); (*blue*) DAPI staining for DNA; experiment was reproduced three times, independently, with similar results.

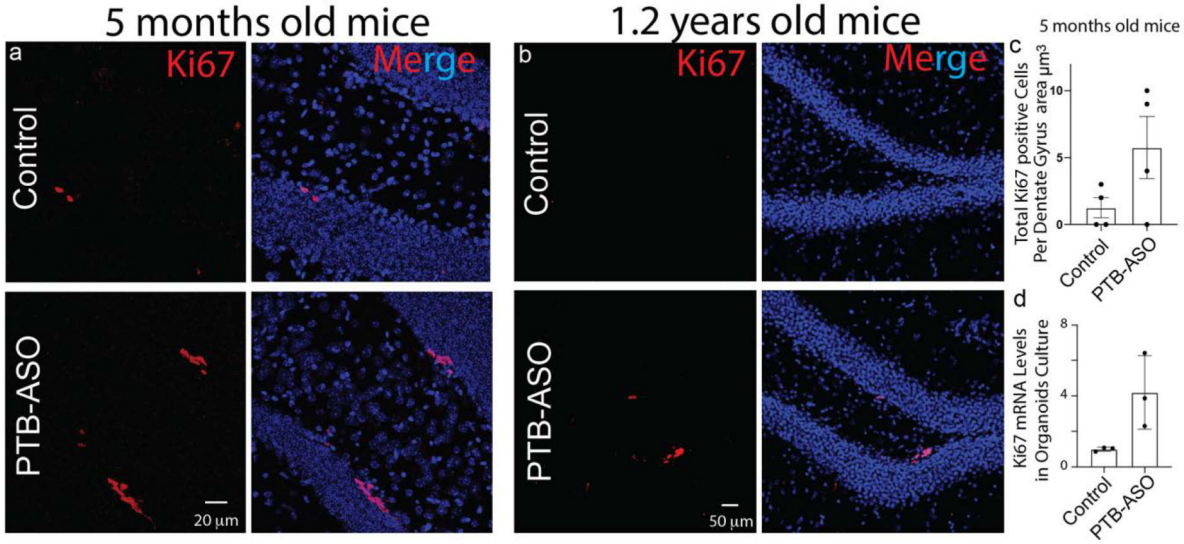

Extended Data Figure 7: ICV delivery of PTB-ASO facilitate Ki67 expression in the mouse dentate gyrus and in human brain organoids.

(a,b) Representative immunofluorescence images from **(a)** 5 months and **(b)** 1.2 years old mouse dentate gyrus taken 2 months post-ICV injection of control ASO or PTB-ASO2. (*Red*) Ki67 (visualized by indirect immunofluorescence); (*blue*) DAPI staining for DNA; experiment was reproduced three times, independently, with similar results.

(c) Total Ki67 positive cells per dentate gyrus of a 5 months old mouse 2 months post ICV delivery of PTB-ASO or control ASO. Data are presented as mean +/− SEM (control: 1.25 +/− 0.75; PTB-ASO mean: 5.75 +/− 2.3; n=4 biological repeats).

(d) Ki67 mRNA levels measured by qPCR, 1 month after the addition of either PTB-ASO2 or control ASO to the human organoid culture medium. Data are presented as fold change mean +/− SEM (control: 1 +/− 0.35; PTB-ASO mean: 4.193 +/− 1.19; n=3 biological repeats).

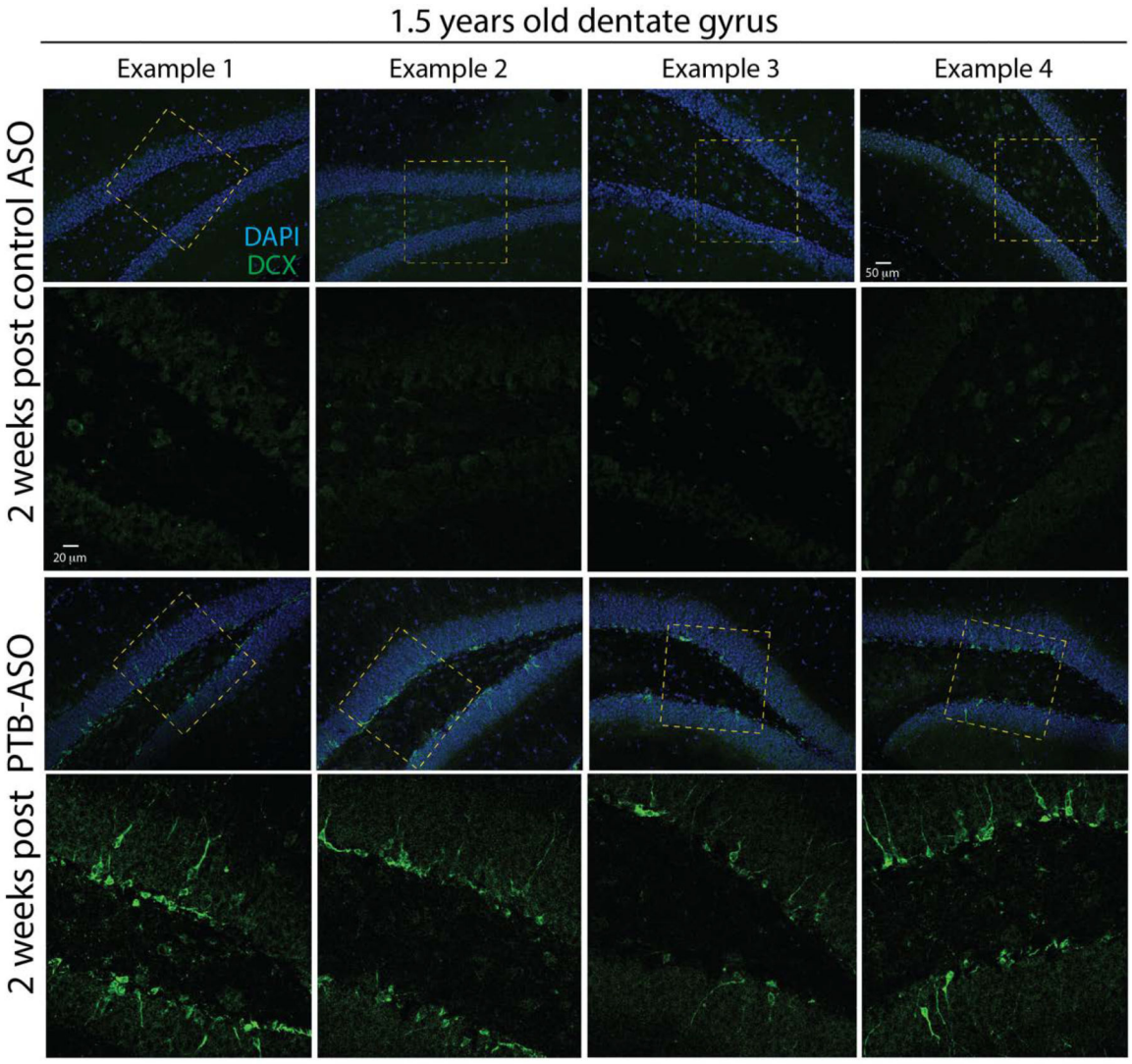

Extended Data Figure 8: DCX expression levels 2 weeks post-PTB-ASO ICV delivery into 1.5 years old mice.

Four representative images and insets of 1.5 years old mice dentate gyrus at 2 weeks post ICV delivery of (*upper*) control or (*lower*) PTB-ASO. (*Green*) DCX (visualized by indirect immunofluorescence); *(blue*) DAPI stain for DNA; experiment was reproduced three times, independently, with similar results.

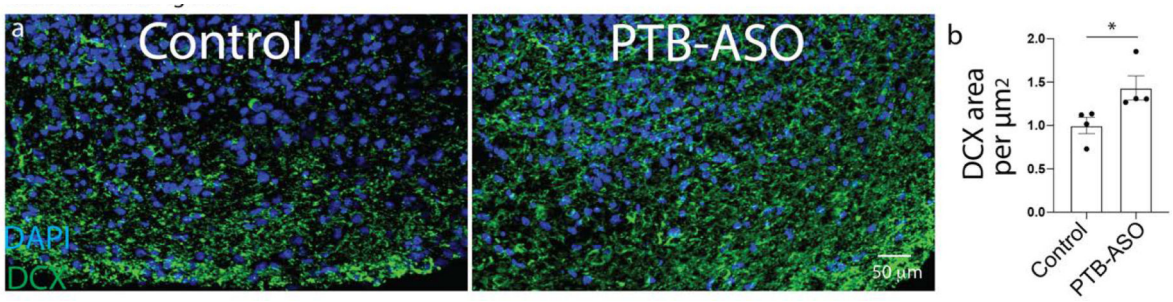

Extended Data Figure 9: DCX protein expression levels 1 month post PTB-ASO treatment in human organoid cultures.

(a) Representative immunofluorescence images of a 5-month-old human organoid taken a 1-month post PTB or control ASO treatment. (*Green*) DCX visualized by indirect immunofluorescence; (*blue*) DAPI to stain DNA; experiment was reproduced four times, independently, with similar results.

(b) Total DCX area in either PTB-ASO or control treated organoids. Data are presented as fold change mean +/− SEM (control: 1 +/− 0.09; PTB-ASO mean: 1.43 +/− 0.13; n=4 biological repeats, two tailed *t* test *p=0.042).

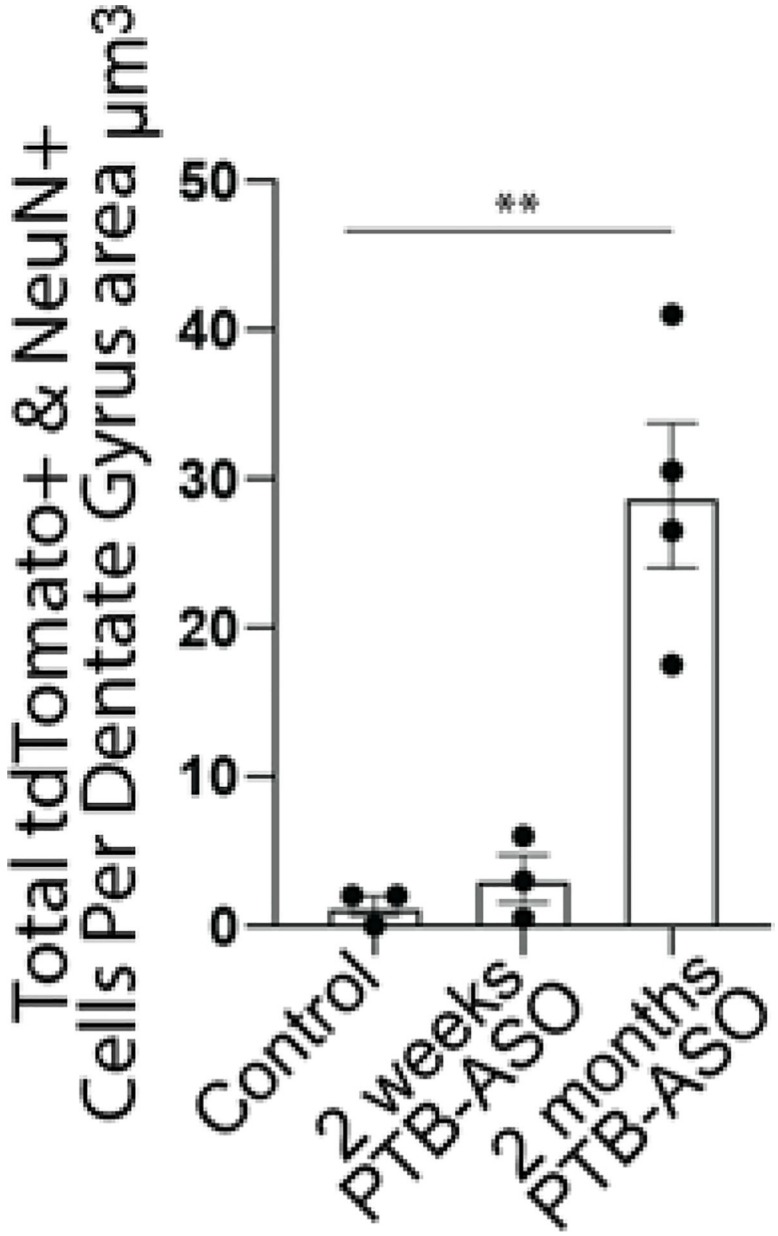

Extended Data Figure 10: tdTomato+, DCX+ cells convert to expression of NeuN within 2 months of PTB ASO injection.

Quantitation of total tdTomato+, NeuN+ positive cells per dentate gyrus area of 5 months old mice 2 weeks or 2 months post PTB-ASO or control ICV injection into mice Data are presented as mean +/− SEM (control: 1.33 +/− 0.66; 2 weeks PTB-ASO mean: 3.16 +/− 1.59; 2 months PTB-ASO mean: 28.88 +/− 4.87; n=3, n=3, n=4, respectively; **, One way ANOVA with Tukey's multiple comparisons, **p=0.0013).

Supplementary Material

Refer to Web version on PubMed Central for supplementary material.

Acknowledgment

This work was supported by a grant from the Nomis Foundation to D.W.C., from grant NS27036 from the N.I.H. to D.W.C. and S.D.C., from a Veteran's Administration grant to T.S.H, and from grants MH109885, MH100175, MH108528, and NS105969 from the NIH to A.R.M. D.W.C. receives salary support from the Ludwig Institute for Cancer Research. R.M. is the recipient of a postdoctoral fellowship from the Hereditary Disease Foundation. We also thank Dr. Amanda Roberts and the mouse phenotyping facility of the Scripps Research Institute for performing the behavioral tests in this manuscript.

Literature Cited:

1. D DB. Degeneration and Regeneration of the Nervous System. Nature 125, 230–231 (1930).
2. Bond AM, Ming GL & Song H Adult Mammalian Neural Stem Cells and Neurogenesis: Five Decades Later. Cell Stem Cell 17, 385–395 (2015). [PubMed: 26431181]
3. Heins N et al. Glial cells generate neurons: The role of the transcription factor Pax6. Nat. Neurosci. 5, 308–315 (2002). [PubMed: 11896398]
4. Kase Y, Kase Y, Shimazaki T & Okano H Current understanding of adult neurogenesis in the mammalian brain: How does adult neurogenesis decrease with age? Inflammation and Regeneration 40, 10 (2020). [PubMed: 32566044]
5. Mertens J, Marchetto MC, Bardy C & Gage FH Evaluating cell reprogramming, differentiation and conversion technologies in neuroscience. Nat. Rev. Neurosci. 17, 424–437 (2016). [PubMed: 27194476]
6. Vierbuchen T et al. Direct conversion of fibroblasts to functional neurons by defined factors. Nature 463, 1035–1041 (2010). [PubMed: 20107439]
7. Barker RA, Götz M & Parmar M New approaches for brain repair - from rescue to reprogramming. Nature 557, 329–334 (2018). [PubMed: 29769670]
8. Qian H et al. Reversing a model of Parkinson ' s disease with in situ converted nigral neurons. Nature 582, 550–556 (2020). [PubMed: 32581380]
9. Zhou H et al. Glia-to-Neuron Conversion by CRISPR-CasRx Alleviates Symptoms of Neurological Disease in Mice. Cell 181, 590–693 (2020). [PubMed: 32272060]
10. Weinberg MS, Criswell HE, Powell SK, Bhatt AP & McCown TJ Viral Vector Reprogramming of Adult Resident Striatal Oligodendrocytes into Functional Neurons. Mol. Ther. 25, 928–934 (2017). [PubMed: 28202388]
11. La Manno G et al. Molecular Diversity of Midbrain Development in Mouse, Human, and Stem Cells. Cell 167, 566–580 (2016). [PubMed: 27716510]
12. Hu J, Qian H, Xue Y & Fu X-D PTB/nPTB: master regulators of neuronal fate in mammals. Biophys. reports 4, 204–214 (2018).
13. Smith RA et al. Antisense oligonucleotide therapy for neurodegenerative disease. J. Clin. Invest. 116, 2290–6 (2006). [PubMed: 16878173]
14. Kordasiewicz HB et al. Sustained Therapeutic Reversal of Huntington's Disease by Transient Repression of Huntingtin Synthesis. Neuron 74, 1031–1044 (2012). [PubMed: 22726834]
15. Finkel RS et al. Nusinersen versus Sham Control in Infantile-Onset Spinal Muscular Atrophy. N. Engl. J. Med. 377, 1723–1732 (2017). [PubMed: 29091570]
16. Miller TM et al. An antisense oligonucleotide against SOD1 delivered intrathecally for patients with SOD1 familial amyotrophic lateral sclerosis: A phase 1, randomised, first-in-man study. Lancet Neurol. 12, 435–442 (2013). [PubMed: 23541756]
17. Miller T et al. Phase 1–2 Trial of Antisense Oligonucleotide Tofersen for SOD1 ALS. N. Engl. J. Med. 383, 109–119 (2020). [PubMed: 32640130]
18. Leavitt BR & Tabrizi SJ Antisense oligonucleotides for neurodegeneration. Science 367, 1428–1429 (2020). [PubMed: 32217715]
19. Vickers TA et al. Efficient reduction of target RNAs by small interfering RNA and RNase H-dependent antisense agents. A comparative analysis. J. Biol. Chem. 278, 7108–7118 (2003). [PubMed: 12500975]

20. Di Lullo E & Kriegstein AR The use of brain organoids to investigate neural development and disease. Nature Reviews Neuroscience 18, 573–584 (2017). [PubMed: 28878372]
21. Trujillo CA et al. Complex Oscillatory Waves Emerging from Cortical Organoids Model Early Human Brain Network Development. Cell Stem Cell 25, 558–569 (2019). [PubMed: 31474560]
22. Madisen L et al. A robust and high-throughput Cre reporting and characterization system for the whole mouse brain. Nat. Neurosci. 13, 133–140 (2010). [PubMed: 20023653]
23. Altman J & Das GD Autoradiographic and histological evidence of postnatal hippocampal neurogenesis in rats. J. Comp. Neurol. 124, 319–335 (1965). [PubMed: 5861717]
24. Ming G li & Song, H. Adult Neurogenesis in the Mammalian Brain: Significant Answers and Significant Questions. Neuron 70, 687–702 (2011). [PubMed: 21609825]
25. Zhao C, Deng W & Gage FH Mechanisms and Functional Implications of Adult Neurogenesis. Cell 132, 645–660 (2008). [PubMed: 18295581]
26. Song H, Berg DA, Bond AM & Ming G. li. Radial glial cells in the adult dentate gyrus: What are they and where do they come from? F1000Research 7, 277 (2018). [PubMed: 29568500]
27. Song H, Stevens CF & Gage FH Astroglia induce neurogenesis from adult neural stem cells. Nature 417, 39–44 (2002). [PubMed: 11986659]
28. Doetsch F, Caille I, Lim DA, Garcia-Verdugo JM & Alvarez-Buylla A Subventricular zone astrocytes are neural stem cells in the adult mammalian brain. Cell 97, 703–716 (1999). [PubMed: 10380923]
29. Morgenstern NA, Lombardi G & Schinder AF Newborn granule cells in the ageing dentate gyrus. J. Physiol. 586, 3751–3757 (2008). [PubMed: 18565998]
30. Sorrells SF et al. Human hippocampal neurogenesis drops sharply in children to undetectable levels in adults. Nature 555, 377–381 (2018). [PubMed: 29513649]
31. Heine VM, Maslam S, Joëls M & Lucassen PJ Prominent decline of newborn cell proliferation, differentiation, and apoptosis in the aging dentate gyrus, in absence of an age-related hypothalamus-pituitary-adrenal axis activation. Neurobiol. Aging 25, 361–375 (2004). [PubMed: 15123342]
32. Schreiner B et al. Astrocyte Depletion Impairs Redox Homeostasis and Triggers Neuronal Loss in the Adult CNS. Cell Rep. 12, 1377–1384 (2015). [PubMed: 26299968]
33. Gerdes J et al. Cell cycle analysis of a cell proliferation-associated human nuclear antigen defined by the monoclonal antibody Ki-67. J. Immunol. 133, 1710–1715 (1984). [PubMed: 6206131]
34. Toni N et al. Neurons born in the adult dentate gyrus form functional synapses with target cells. Nat. Neurosci. 11, 901–907 (2008). [PubMed: 18622400]
35. Zhao C, Teng EM, Summers RG, Ming GL & Gage FH Distinct morphological stages of dentate granule neuron maturation in the adult mouse hippocampus. J. Neurosci. 26, 3–11 (2006). [PubMed: 16399667]
36. Deng W, Aimone JB & Gage FH New neurons and new memories: How does adult hippocampal neurogenesis affect learning and memory? Nature Reviews Neuroscience 11, 339–350 (2010). [PubMed: 20354534]
37. Van Praag H et al. Functional neurogenesis in the adult hippocampus. Nature 415, 1030–1034 (2002). [PubMed: 11875571]
38. Kosik KS & Finch EA MAP2 and tau segregate into dendritic and axonal domains after the elaboration of morphologically distinct neurites: an immunocytochemical study of cultured rat cerebrum. J. Neurosci. 7, 3142–3153 (1987). [PubMed: 2444675]
39. Altman J & Bayer SA Migration and distribution of two populations of hippocampal granule cell precursors during the perinatal and postnatal periods. J. Comp. Neurol. 301, 365–381 (1990). [PubMed: 2262596]
40. Kempermann G, Song H & Gage FH Neurogenesis in the Adult Hippocampus. Cold Spring Harb. Perspect. Biol. 7, 9 (2015).
41. Wang L-L, Garcia CS, Zhong X, Ma S & Zhang C-L Rapid and efficient in vivo astrocyte-to-neuron conversion with regional identity and connectivity? bioRxiv 2020.08.16.253195 (2020)
42. Eliasson C et al. Intermediate filament protein partnership in astrocytes. J. Biol. Chem. 274, 23996–24006 (1999). [PubMed: 10446168]

43. Van Praag H, Kempermann G & Gage FH Running increases cell proliferation and neurogenesis in the adult mouse dentate gyrus. Nat. Neurosci. 2, 266–270 (1999). [PubMed: 10195220]

44. Barnes CA Memory deficits associated with senescence: a neurophysiological and behavioral study in the rat. J. Comp. Physiol. Psychol. 93, 74–104 (1979). [PubMed: 221551]

45. Heyser CJ & Chemero A Novel object exploration in mice: not all objects are created equal. Behav. Processes 89, 232–238 (2012). [PubMed: 22183090]

46. Crawley JN Behavioral phenotyping of transgenic and knockout mice: experimental design and evaluation of general health, sensory functions, motor abilities, and specific behavioral tests. Brain Res. 835, 18–26 (1999). [PubMed: 10448192]

47. Gage FH Mammalian neural stem cells. Science 287, 1433–1438 (2000). [PubMed: 10688783]

48. Bennett CF, Krainer AR & Cleveland DW Antisense Oligonucleotide Therapies for Neurodegenerative Diseases. Annu. Rev. Neurosci. 42, 385–406 (2019). [PubMed: 31283897]

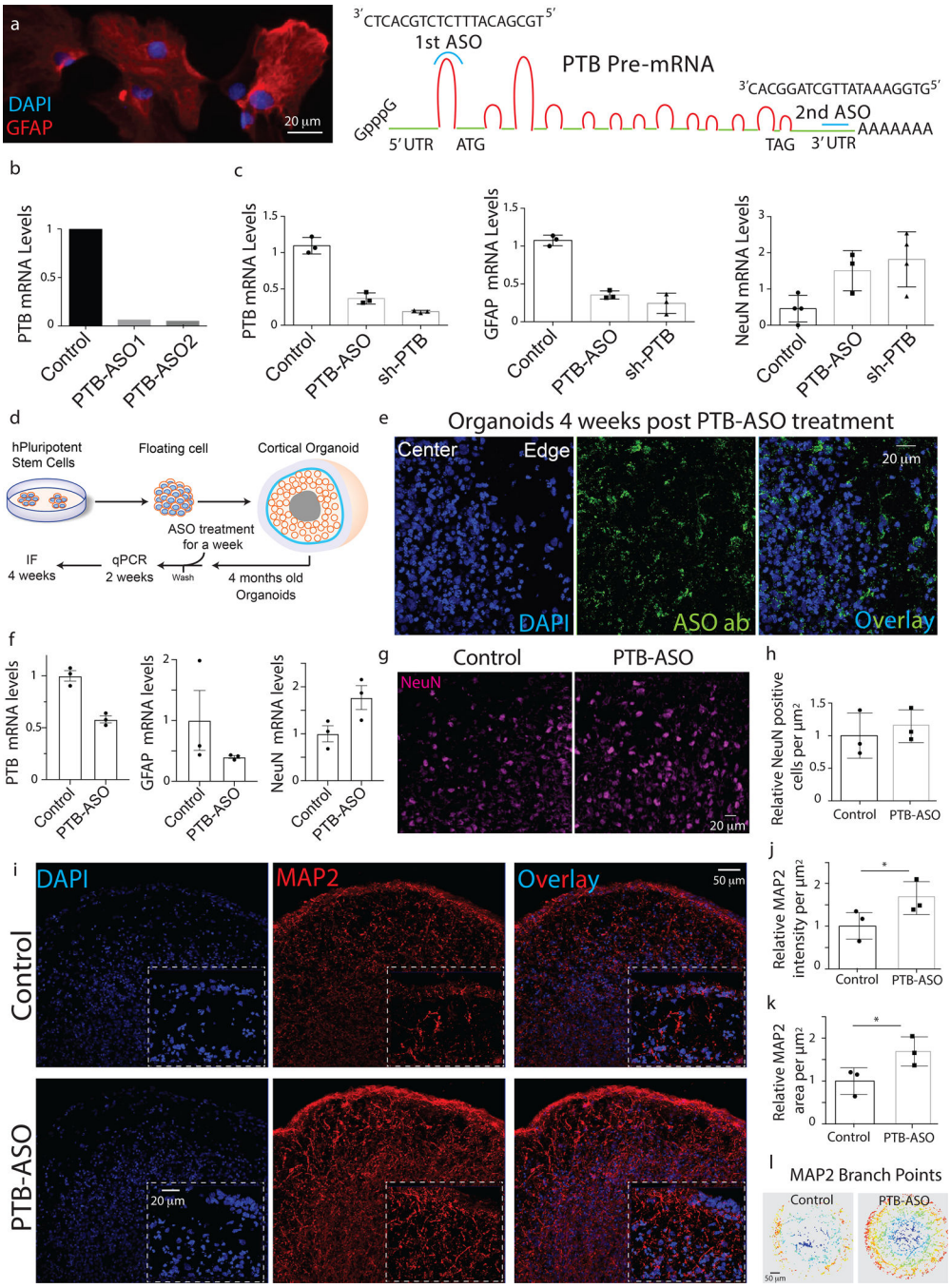

Figure 1: Application of an ASO catalyzing PTB mRNA degradation is sufficient to induce new neurons in a mature human organoid model.

(a) (*Left panel*) - Representative image of mouse astrocytes in culture performed to identify an efficient reduction in PTB mRNA levels using either of two ASOs targeting the PTB pre-mRNA or mRNA or by transduction with a lentivirus encoding an shRNA to PTB; experiment was reproduced three times independently with similar results. (*Right panel*) Positions and sequences of the PTB ASOs 1 and 2 are marked with blue bars on the PTB pre-mRNA. Green lines represent PTB exons, Red lines represent PTB introns.

(b) PTB RNA levels measured by qPCR, 3 days after transfection of a murine mammary cell line (4T1) with either of two most effective PTB-ASOs identified from a screen of ~200 potential ASOs. Experiment performed once for validation purposes of larger hit screen. Further validation performed in murine astrocyte cultures as shown in (c) below. Data are presented as fold change from control (Control=1, PTB-ASO1=0.06, PTB-ASO2=0.05)
(c) PTB, GFAP, or NeuN mRNA levels measured by qPCR 3 days after addition to an astrocyte culture of either PTB-ASO2 or transduction with lentiviral-shRNA-PTB; Data are presented as mean fold change +/− SEM. (*Left* graph for PTB mRNA: control mean: 1 +/− 0.06; PTB-ASO mean: 0.36 +/−0.04; LV-PTB mean: 0.18 +/−0.01, n=3 biological repeats, one way ANOVA with Tukey's multiple comparisons **p<0.0001; *Middle* graph for GFAP mRNA: control mean: 1 +/− 0.04; PTB-ASO mean: 0.35 +/− 0.03; LV-PTB mean: 0.24 +/ −0.07, n=3 biological repeats, one way ANOVA with Tukey's multiple comparisons **p<0.0001; *Right* graph - for NeuN mRNA: control mean: 0.45 +/− 0.18; PTB-ASO mean: 1.5 +/− 0.32; LV-PTB mean: 1.8 +/−0.38, n=3,n=4 biological repeats, one way ANOVA with Tukey's multiple comparisons *p=0.027);
(d) Schematic of the organoid culture procedure and experimental timeline used in parts **e-l**.
(e) Representative immunofluorescence images from 5-month-old human organoid taken 1-month post-PTB-ASO2 addition to the organoid culture medium. (*Green*) PTB-ASO visualized by indirect immunofluorescence; (*blue*) DAPI staining for DNA; experiment was reproduced in three biological samples with similar results.
(f) PTB, GFAP, or NeuN mRNA levels measured by qPCR 2 weeks after the addition of either PTB-ASO2 or control to the human organoid culture medium; n=3 biological replications in each graph. Data are presented as mean fold change +/− SEM. (*Left* graph: control mean: 1 +/− 0.05; PTB-ASO mean: 0.58 +/−0.03; two-tailed *t* test, **P=0.002. *Middle* graph: control mean: 1 +/− 0.49; PTB-ASO mean: 0.39 +/− 0.02; two-tailed *t* test, P=0.2.; *Right* graph - control mean: 1+/−0.17; PTB-ASO mean 1.76+/− 0.25; two-tailed *t* test, P=0.06).
(g) Representative immunofluorescence images from a 5-month-old human organoid taken 1-month post-PTB-ASO2 application to the culture medium. High magnification images show a view of (*magenta*) NeuN (visualized by direct immunofluorescence); experiment was reproduced in three biological samples with similar results.
(h) Quantification of total NeuN positive cells in a whole organoid 4 weeks following treatment with PTB-ASO2 compared to a control non-targeting ASO. n=3 biological replications. Data are presented as mean fold change +/− SEM (control mean: 1+/−0.25; PTB-ASO mean: 1.2+/−0.14).
(i) Representative immunofluorescence images of a 5-month-old human organoid taken 1-month post-PTB-ASO2 or control treatment. Insets show higher magnification images visualized with (*red*) the dendritic marker MAP2 or (*blue*) DAPI to stain DNA; experiment was reproduced in three biological repeats with similar results.
(j,k) Total MAP2 **(j)** intensity and **(k)** area in either PTB-ASO or control-treated organoids. Data are presented as mean fold change +/− SEM. (control mean intensity: 1+/−0.17; PTB-ASO mean: 1.68+/−0.22 control mean area: 1+/−0.15; PTB-ASO mean: 1.71+/−0.19, n=3, n=3; one-tailed *t* test; *p=0.036, *p=0.029, respectively).

(l) Representation images of Sholl analysis to identify dendritic branch points in organoids treated with PTB-ASO or control. Images were generated for three biological samples with similar results.

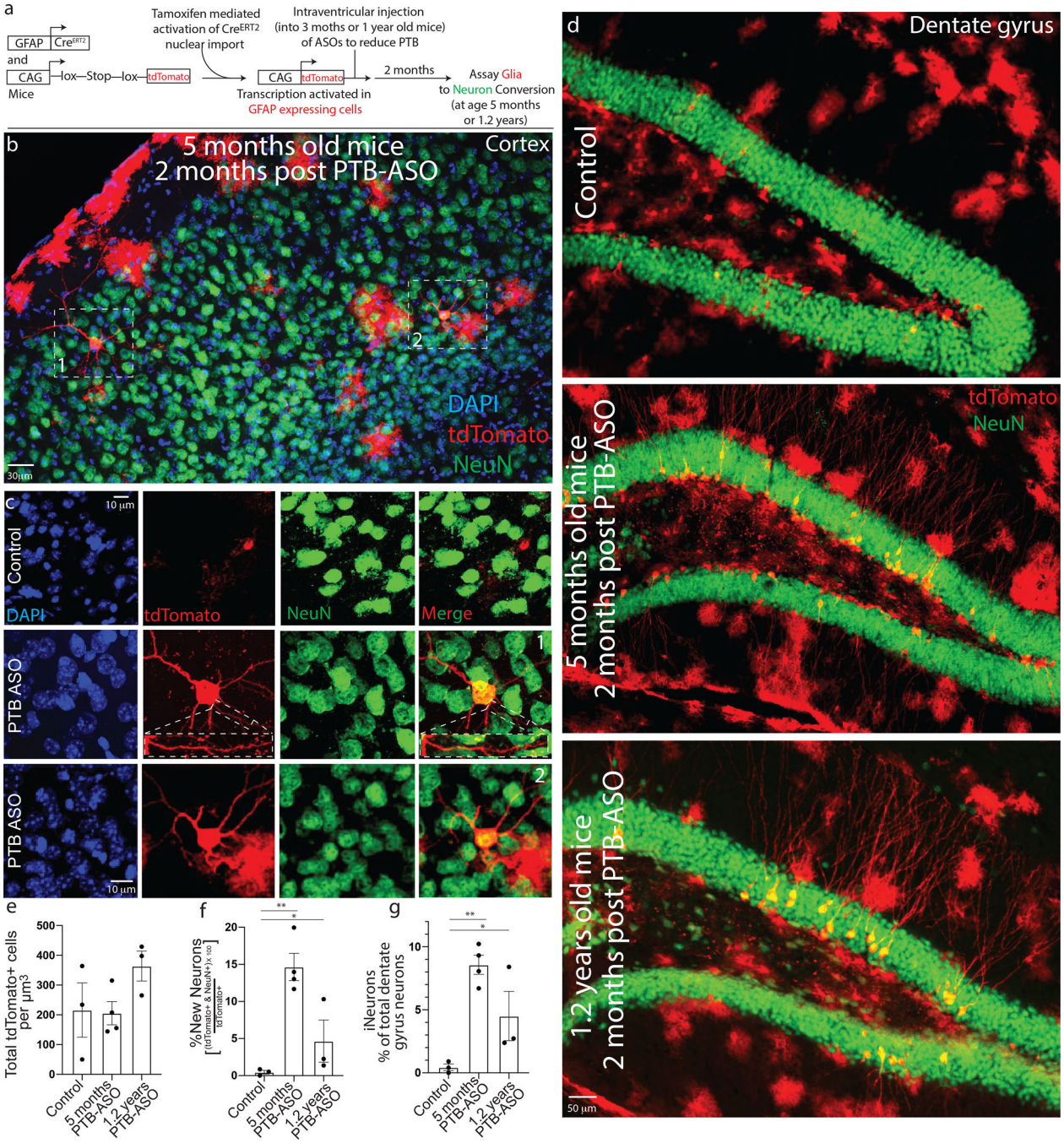

Figure 2: Injection of an ASO into the cerebral spinal fluid to suppress PTB is sufficient to induce new neurons in the adult and aged mouse brain.

(a) Schematic of the experimental strategy used to mark GFAP positive cells with the red fluorescent protein tdTomato and to follow conversion into neurons in the adult mouse brain after intraventricular (ICV) injection of a PTB targeting ASO into either 3-months-old or 1-year-old mouse carrying a tamoxifen-inducible GFAP-Cre^{ERT2} transgene and a modified chicken beta-actin (CAG) promoted lox-Stop-lox tdTomato gene integrated at the Rosa locus.

(b,c) Representative immunofluorescence image **(b)** from 5 months old mouse cortex taken 2 months post-ICV injection of control or PTB-ASO2 into mice carrying both a CAG-lox-stop-lox-tdTomato gene and a tamoxifen-inducible GFAP-Cre^{ERT2} transgene. **(c)** Insets show high-magnification views of newly induced neurons expressing (*green*) NeuN and (*red*) tdTomato (visualized by direct immunofluorescence and direct fluorescence, respectively); (*blue*) DAPI staining for DNA; experiment was reproduced three times, independently, with similar results.

(d) Representative immunofluorescence images from mouse dentate gyrus taken 2 months post-ICV injection of control or PTB-ASO2 into 3 months old and 1 year old mice carrying both a CAG-lox-stop-lox-tdTomato gene and a tamoxifen-inducible GFAP-Cre^{ERT2} transgene. (iNeurons) expressing (*green*) NeuN and (*red*) tdTomato (visualized by direct immunofluorescence and direct fluorescence, respectively); experiment was reproduced three times in control and aged mice and four times in 5 months old mice, independently, with similar results.

(*e*) Total tdTomato expressing cells and **(f)** the percentage of tdTomato expressing cells converted into neurons, as determined by their accumulation of NeuN at 5 months and 1.2 years old of age. Data are presented as mean +/− SEM (For **e** - control mean: 216+/−91.09; 5 months PTB-ASO mean: 205.6+/−38.96; 1.2 years old PTB-ASO mean: 363.8+/−50.25; n=3, n=4, n=3 biological repeats. For **f** - control mean: 1% +/−0.57%; 5 months PTB-ASO mean: 14.31%+/−2.33%; 1.2 years old PTB-ASO mean: 5.33%+/−2.58%; n=3, n=4, n=3 biological repeats; one-way ANOVA with Tukey's multiple comparisons **p=0.0032, *p=0.048).

(g) Percentage of the total induced neurons (iNeurons) out of total neurons in granular cell layer of the dentate gyrus, 2 months after ICV injection of saline or PTB-ASO2 at 5 months and 1.2 years old mice. Data are presented as mean +/− SEM (control mean: 0.43% +/−0.26%; 5 months PTB-ASO mean: 8.58%+/−0.76%; 1.2 years old PTB-ASO mean: 4.5% +/−1.95%; n=3, n=4, n=3 biological repeats; one way ANOVA with Tukey's multiple comparisons **p=0.0017, *p=0.047.

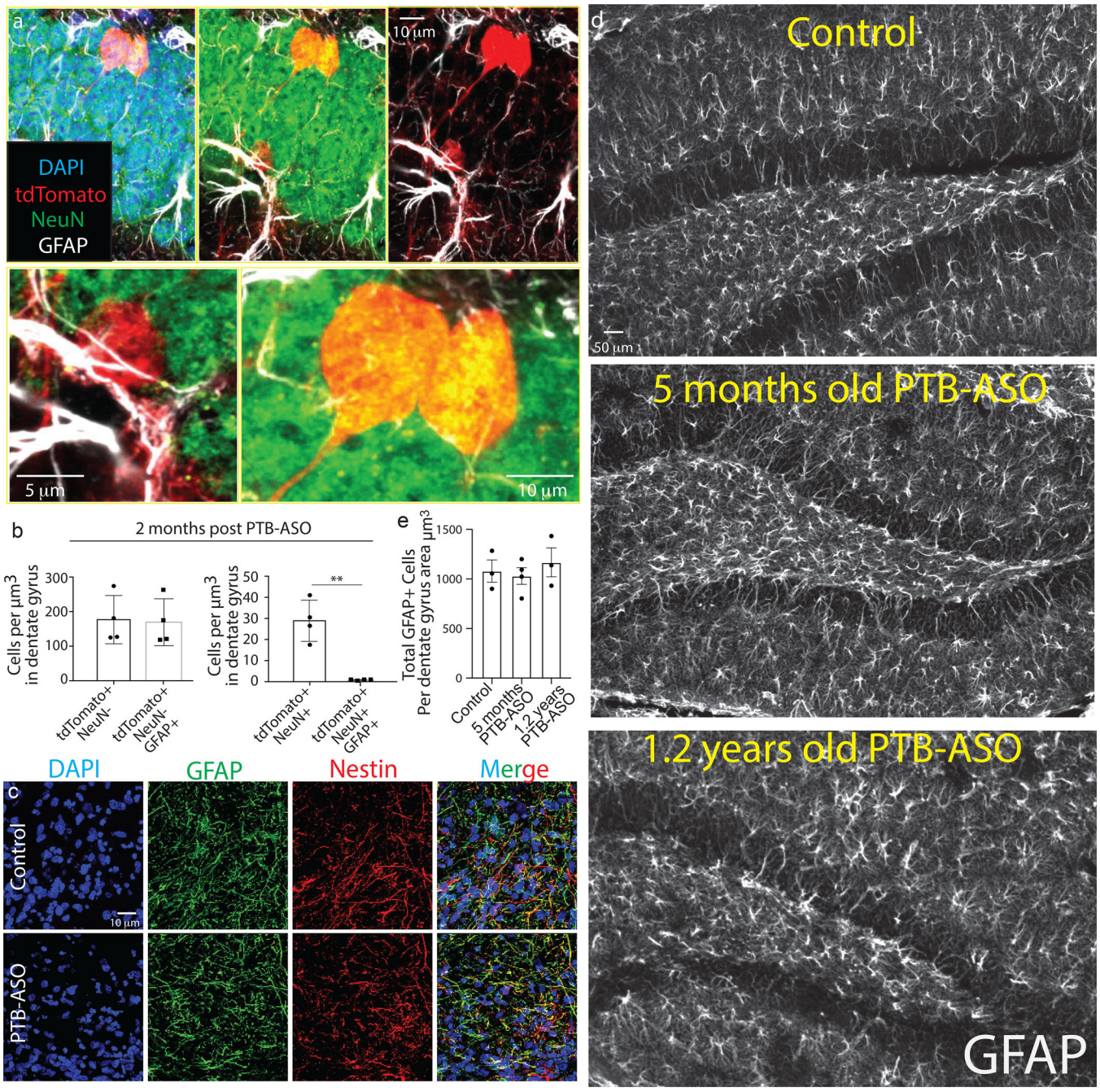

Figure 3: Transition of GFAP:tdTomato+ cells into new neurons results in no depletion in the total GFAP cell number.

(**a**) Higher magnification views of newly induced neurons (iNeurons) expressing (*green*) NeuN and (*red*) tdTomato (NeuN visualized by direct immunofluorescence and tdTomato by direct fluorescence); (*blue*) DAPI staining for DNA; (*white*) GFAP visualized by indirect immunofluorescence; experiment was reproduced four times, independently, with similar results.

(b) Total number of (*left*) tdTomato+ and NeuN- or *(right)* tdTomato+ and NeuN+ expressing cells, either with or without GFAP labeling, per dentate gyrus, 2 months post

ICV injection of PTB-ASO. Data are presented as mean +/− SEM (*left*: tdTomato/NeuN: 176.8+/− 34.92; tdTomato/NeuN/GFAP mean: 167 +/− 34.32; *right*: tdTomato/NeuN mean: 28.88 +/− 4.87; tdTomato/NeuN/GFAP mean: 0.87 +/− 0.12; n=4 biological repeats; two tailed *t* test **p=0.0012)

(c) Representative images of human organoids 1 month post PTB-ASO or control-ASO application in the growth media (*green*) GFAP and (*red*) Nestin (both visualized by direct immunofluorescence); *(blue*) DAPI staining for DNA; experiment was reproduced three times, independently, with similar results.

(d) Representative images of a dentate gyrus taken 2 months post intracerebroventricular (ICV) injection of control or PTB-ASO2 into 3-month-old and 1-year old mice; (*white*) GFAP visualized by indirect immunofluorescence; experiment was reproduced three times, for control and aged mice and four times for five months old mice, independently, with similar results.

(e) Total GFAP positive cells per dentate gyrus area of 5 months and 1.2 years old PTB-ASO or control injected mice. Data are presented as mean +/− SEM (control mean: 1074+/−83.55; 5 months PTB-ASO mean: 1006+/−82.45; 1.2 years old PTB-ASO mean: 1214+/−104.8; n=3, n=4, n=3 biological repeats).

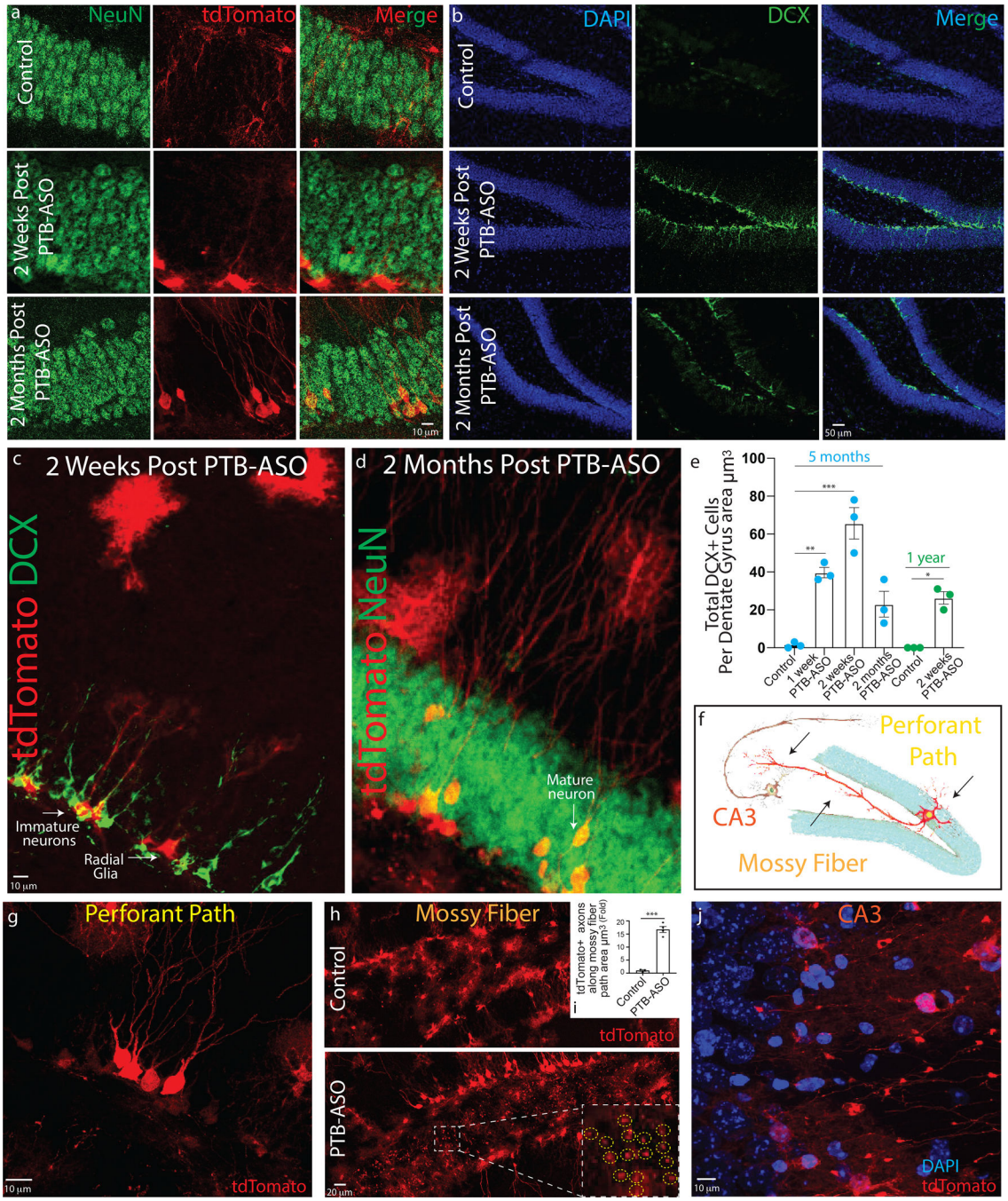

Figure 4: Newly generated neurons follow canonical neurogenesis in the dentate gyrus.

(a) Representative images of 5 months old mice dentate gyrus of control or PTB-ASO2 at 2 weeks and 2 months post ICV delivery. *(green)* NeuN and (*red*) tdTomato (NeuN visualized by direct immunofluorescence and tdTomato by direct fluorescence); experiment was reproduced three times, independently, with similar results.

(b) Representative images of 5 months old mice dentate gyrus at 2 weeks and 2 months post ICV delivery of control or PTB-ASO2. *(blue)* DAPI and (*green*) DCX (visualized by direct

immunofluorescence); experiment was reproduced three times for control and 2 weeks time points and four times in 2 months time point, independently, with similar results.

(c,d) Higher magnification views of newly induced neurons (iNeurons) at 2 weeks or 2 months post ICV delivery of PTB-ASO2 expressing **(c)** (*green*) DCX and (*red*) tdTomato and **(d)** (*green*) NeuN and (*red*) tdTomato 2 months post PTB-ASO ICV injection; experiment was reproduced three times, independently, with similar results.

(e) Total DCX positive cells per dentate gyrus area of 5 months and 1 year old mice, over a two month period post PTB-ASO or control injected mice. Data are presented as mean +/− SEM (control mean: 1.33+/−0.88; 5 months, 1 week PTB-ASO mean: 39.67+/−2.72; 5 months, 2 week PTB-ASO mean: 65.67+/−8.25; 5 months, 2 months PTB-ASO mean: 23+/−86.8; aged mice control mean: 0+/−0; aged mice PTB-ASO mean: 26.33+/−3.28; n=3 biological repeats. One-way ANOVA with Tukey's multiple comparisons **p=0.001, ***p<0.0001, *p=0.0185).

(f) Illustration of mice hippocampus major substructural areas marked with a color code; (*yellow*) Perforant path (*orange*) mossy fiber (*red*) CA3

(g) High magnification view of the newly induced neurons sending their neurites into the Perforant path of a 5-month-old mouse taken 2 months post-ICV injection of PTB-ASO. (*Red*) tdTomato visualized by direct fluorescence; experiment was reproduced four times, independently, with similar results.

(h) Representative images of tdTomato+ axons in part of the mossy fiber path of a 5-month-old mouse taken 2 months post-ICV injection of *(upper)* control or *(lower)* PTB ASO into 3-month-old mice carrying both a CAG-lox-stop-lox-tdTomato gene (integrated at the *Rosa* locus) and a tamoxifen-inducible GFAP-Cre^{ERT2} transgene. Inset shows a representative high-magnification view of tdTomato+ axons (*circled*) that were counted. (*Red*) tdTomato visualized by direct fluorescence; experiment was reproduced four times, independently, with similar results.

(i) Fold increase in tdTomato+ axons in the mossy fiber area of PTB-ASO treated animals over control animals; Data are presented as mean +/− SEM. (control mean: 1 +/− 0.31; PTB-ASO mean: 16.71 +/− 1.156; n=3, n=4 biological repeats; two tailed *t* test ***p<0.0001)

(j) High magnification view of tdTomato+ axons in part of the hippocampal CA3 area 2 months post ICV delivery of PTB-ASO2 into CSF. *(Red)* tdTomato visualized by direct fluorescence; (*blue*) DAPI staining for DNA. experiment was reproduced four times, independently, with similar results.

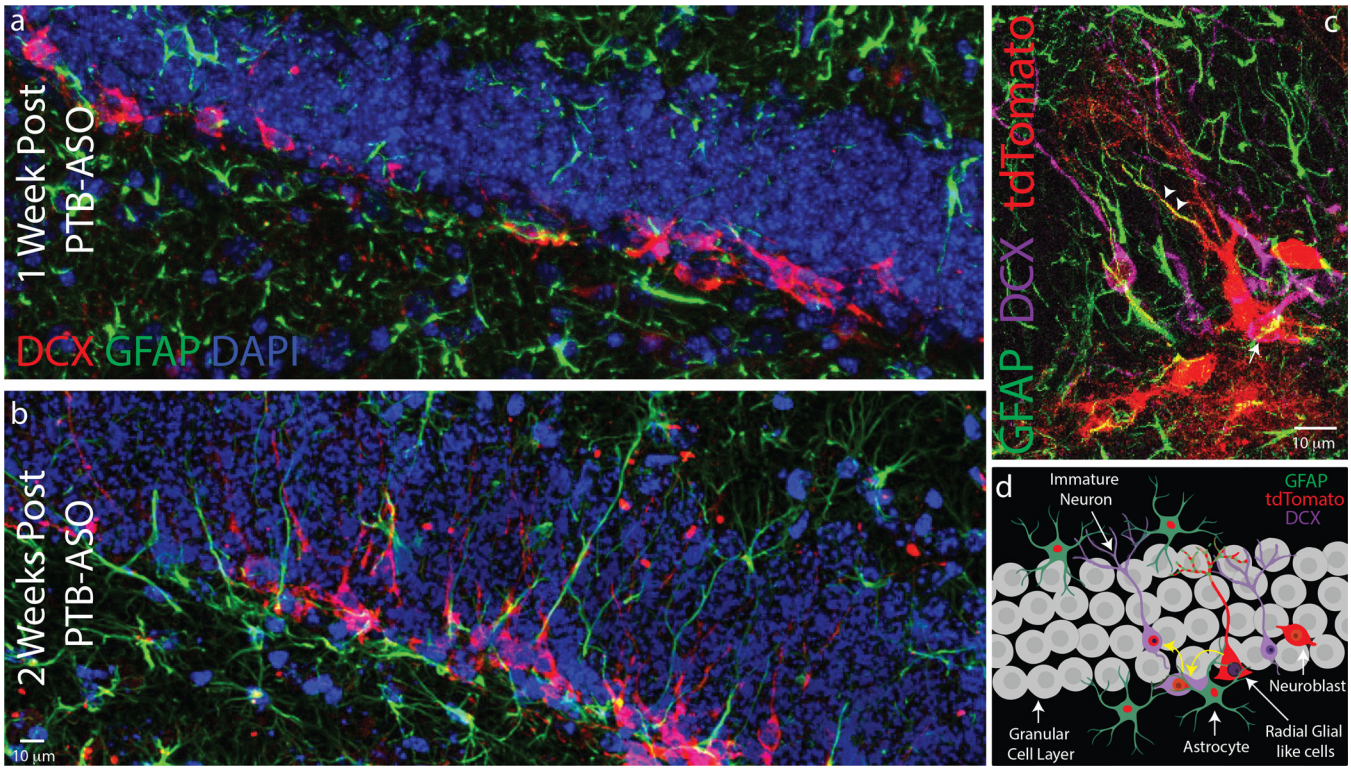

Figure 5: Radial glial-like cells are the main cell origin for new generated neurons in dentate gyrus, post PTB reduction using ASO.

(a,b) Representative images of 3 months old mice dentate gyrus at **(a)** 1 week and **(b)** 2 weeks post ICV delivery of PTB-ASO. (*green*) GFAP and (red) DCX, each visualized by indirect immunofluorescence. *(Blue*) DAPI; experiment was reproduced three times, independently, with similar results.

(c) Representative image of 3 months old mice dentate gyrus at 1 week post ICV delivery of PTB-ASO. (*Green*) GFAP and (*magenta*) DCX (visualized by indirect immunofluorescence). (R*ed*) tdTomato (visualized by direct fluorescence); experiment was reproduced three times, independently, with similar results.

(d) Visual representation for neuronal conversion in the dentate gyrus post PTB reduction using ASOs, created with BioRender.com.

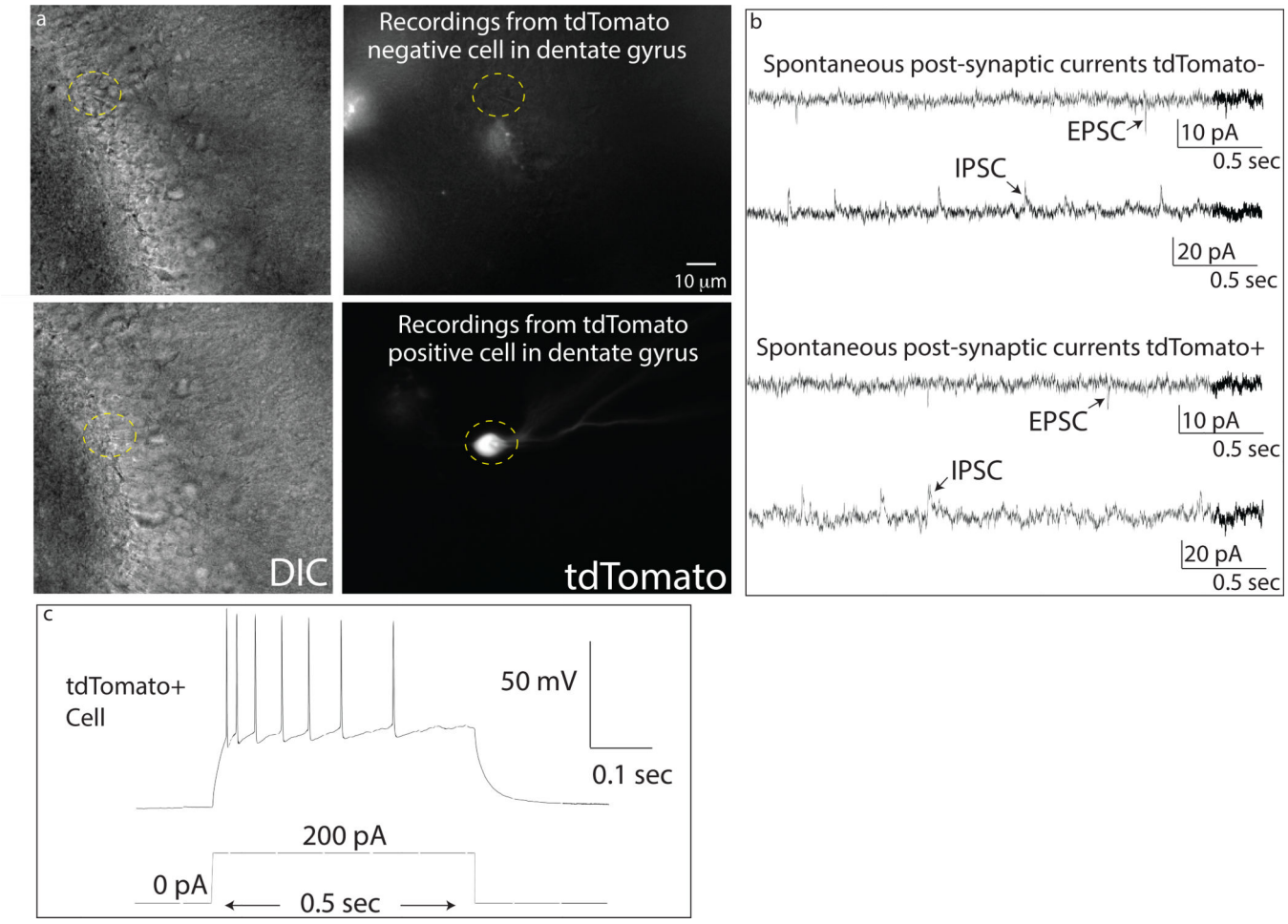

Figure 6: Newly generated neurons have intrinsic membrane properties of mature granular neurons

(a) Representative DIC and fluorescence images of a tdTomato negative and tdTomato positive cell located in the granule cell layer of the dentate gyrus; We analyzed total of 5 tdTomato negative and 7 tdTomato positive neurons; experiment was reproduced three times, independently, with similar results.

(b) Representative current recordings from *(upper)* tdTomato negative and *(lower)* tdTomato positive cells in the granular cell layer. sEPSCs and sIPSCs in tdTomato negative and tdTomato positive cells were recorded. We analyzed total of 5 tdTomato negative and 7 tdTomato positive neurons; experiment was reproduced three times, independently, with similar results.

(c) Action potentials in a tdTomato positive cell in response to the current step. We analyzed total tdTomato positive neurons; experiment was reproduced three times, independently, with similar results.

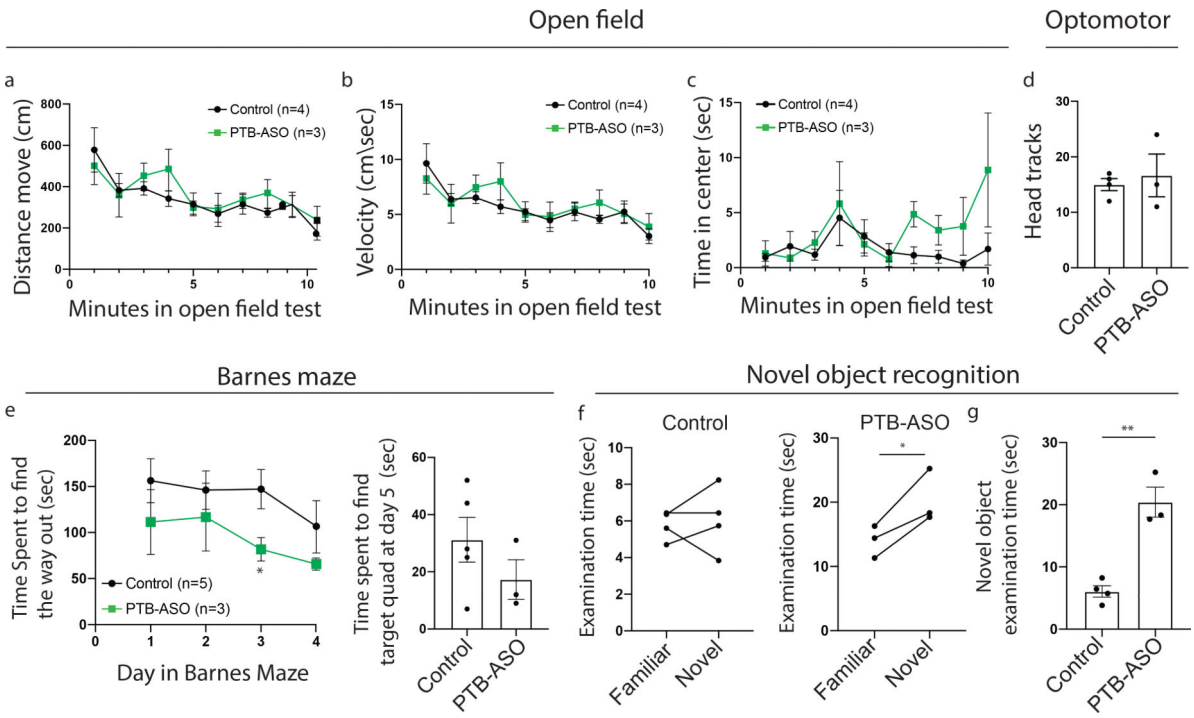

Figure 7: Generation of new functional neurons in aged mouse dentate gyrus.

(a,b,c) Measurements of **(a)** distance, **(b)** velocity and **(c)** time spent in center, in open field test of 1.5 year old mice injected with control or PTB ASOs. Data are presented as mean +/− SEM. (n=4 in control group, n=3 in PTB-ASO injected group)

(d) Quantification of total head movements of 1.5 year old mice injected with control or PTB ASO following light cues in an optomotor test. Data are presented as mean +/− SEM (control mean: 15 +/− 1.08; PTB-ASO mean: 16.67 +/− 3.84 n=4, n=3 biological repeats).

(e) *(left)* Barnes maze training plot of 1.5 year old mice analyzed 2 months post ICV injection with control or PTB-ASO, during 4 days of practice. Data are presented as mean +/− SEM. (n=5, n=3 respectively; two-way ANOVA, *p=0.02) (*Right)* Quantification of the time required to find target quadrant on the fifth day of Barnes maze assay in PTB-ASO or control mice. Data are presented as mean +/− SEM (control mean: 31.20 +/− 7.84; PTB-ASO mean: 17.33 +/− 6.88; n=5, n=3 biological repeats).

(f,g) Quantification of the time spent near familiar and novel object in control-ASO or PTB-ASO 1.5 year injected mice plotted for **(f)** an individual mouse or for **(g)** the average of each group. For **f** Data are presented as individual mice. n=4, n=3, two tailed paired t test *p=0.047 for **g** - Data are presented as mean +/− SEM. (control mean: 6.07 +/− 0.91; PTB-ASO mean: 20.43 +/− 2.41; n=4,n=3 biological repeats; respectively; two tailed t test **p=0.0015)

Table 1:

Comparison table of membrane properties between tdTomato negative and tdTomato positive cells

Intrinsic properties (n=5 negatives, 7 positives)			
	tdTomato−	**tdTomato+**	**P Value**
resting membrane potential (mV)	−74.96±1.08	−73.85±1.72	0.63
input resistance (MΩ)	316.08±20.60	300.37± 20.24	0.61
action potential threshold (mV)	−28.77±2.10	−30.03±1.10	0.58
action potential half-width (ms)	1.27±0.04	1.30±0.05	0.72
capacitance (pF)(n=5,6)	111.13±11.68	98.95 ±14.21	0.53

Comparison table of membrane properties between tdTomato negative and tdTomato positive cells; experiment was reproduced three times, independently, with similar results.